The HCV Envelope Glycoprotein Down-Modulates NF-κB Signalling and Associates With Stimulation of the Host Endoplasmic Reticulum Stress Pathway

Lindsay G. A. McKay[1†‡], Jordan Thomas[1‡], Wejdan Albalawi[1], Antoine Fattaccioli[2], Marc Dieu[3], Alessandra Ruggiero[1†], Jane A. McKeating[4], Jonathan K. Ball[5], Alexander W. Tarr[5], Patricia Renard[2,3], Georgios Pollakis[1] and William A. Paxton[1*]

[1] Department of Clinical Infection, Microbiology and Immunology, Institute of Veterinary and Ecological Sciences, University of Liverpool, Liverpool, United Kingdom, [2] Laboratory of Biochemistry and Cell Biology (URBC), Namur Research Institute for Life Sciences (NARILIS), University of Namur (UNamur), Namur, Belgium, [3] MaSUN, Mass Spectrometry Facility, University of Namur (UNamur), Namur, Belgium, [4] Nuffield Department of Medicine, University of Oxford, Oxford, United Kingdom, [5] Wolfson Centre for Global Virus Research and School of Life Sciences, University of Nottingham, Nottingham, United Kingdom

Following acute HCV infection, the virus establishes a chronic disease in the majority of patients whilst few individuals clear the infection spontaneously. The precise mechanisms that determine chronic HCV infection or spontaneous clearance are not completely understood but are proposed to be driven by host and viral genetic factors as well as HCV encoded immunomodulatory proteins. Using the HIV-1 LTR as a tool to measure NF-κB activity, we identified that the HCV E1E2 glycoproteins and more so the E2 protein down-modulates HIV-1 LTR activation in 293T, TZM-bl and the more physiologically relevant Huh7 liver derived cell line. We demonstrate this effect is specifically mediated through inhibiting NF-κB binding to the LTR and show that this effect was conserved for all HCV genotypes tested. Transcriptomic analysis of 293T cells expressing the HCV glycoproteins identified E1E2 mediated stimulation of the endoplasmic reticulum (ER) stress response pathway and upregulation of stress response genes such as ATF3. Through shRNA mediated inhibition of ATF3, one of the components, we observed that E1E2 mediated inhibitory effects on HIV-1 LTR activity was alleviated. Our *in vitro* studies demonstrate that HCV Env glycoprotein activates host ER Stress Pathways known to inhibit NF-κB activity. This has potential implications for understanding HCV induced immune activation as well as oncogenesis.

Keywords: immunity, HIV-LTR, HCV, NF-κB, endoplasmic reticulum stress

INTRODUCTION

Hepatitis C Virus (HCV) is a member of the *Flaviviridae* family which infects approximately 58 million people worldwide and can mediate severe hepatic injury and progressive liver fibrosis through stimulating persistent inflammation and oxidative stress (1–5). Approximately 50-80% of HCV positive individuals fail to resolve the infection whilst the remaining patients spontaneously

clear virus within 6 months, though the mechanisms that determine either of these outcomes are incompletely understood (6–9). Several factors are associated with increased likelihood of chronic HCV infection including a higher diversity of HCV quasispecies (10), ethnicity of the host (9, 11, 12) and co-infection with Human Immunodeficiency Virus Type 1 (HIV-1) (13–15). Conversely, factors such as sexual transmission (16), Interleukin 28-B (IL28B) genotype CC (17–19), several Human Leukocyte Antigen (HLA) types including HLA-B*57, female sex and the strength of HCV specific T cell responses are associated with increased likelihood of spontaneous clearance (20, 21).

HCV encoded immunomodulatory factors have been proposed to influence the establishment of chronic infection by interfering with intracellular innate immunity pathways (22). For example, it has been suggested that the HCV core protein modulates cellular immune responses *via* downregulation of Nuclear Factor Kappa-Light-Chain-Enhancer of Activated B Cells (NF-κB) activation (23–25), inhibition of Interleukin 2 (IL-2) production (26) and suppression of CD8+ and CD4+ T cell responses (27, 28). Similarly, the HCV NS2 and NS3/4A proteins down-modulate early innate immune responses by inhibiting key steps in type 1 Interferon (IFN) signalling pathways *in vitro* (29–32) and *in vivo* (33). Additionally, infection with HCV may down-modulate cellular immune responses indirectly, through upregulation of stress responses. Infection with HCV *in vitro* stimulates endoplasmic reticulum (ER) stress and leads to the induction of the Unfolded Protein Response (UPR) and autophagy. These cryoprotective responses function to resolve ER stress by reducing protein synthesis and increasing the protein processing capacity of the infected cell (34–36). Nevertheless, upregulation of ER stress has been proposed to promote HCV replication (37–39) and also down-modulate innate immune signalling in the infected cell (36), providing a favourable landscape for HCV replication and potentially aiding the establishment of chronic infection. Several reports have identified that individual proteins of HCV are potent activators of the UPR independent of HCV replication, including the envelope (Env) glycoproteins E1 and E2 (40–42). Both E1 and E2 are highly glycosylated type 1 transmembrane glycoproteins which use membrane anchored C-terminal tails to remain tethered in the endoplasmic reticulum (ER) prior to a series of protein maturation events (43). Currently, there is limited understanding regarding the molecular mechanisms through which HCV Env glycoproteins may modulate cellular immune responses and contribute to HCV mediated immune regulation.

Here we studied the interaction between the HCV Env glycoprotein and its effects on modulating HIV-1 Long Terminal Repeat (LTR) activation as a tool to measure the effects of these proteins on NF-κB signalling in 293T, TZM-bl and the more physiologically relevant Huh7 cell line. Using plasmids that express HIV-1 or luciferase under the control of the HIV-1 LTR, we investigated the ability of HCV Env glycoprotein to modulate cellular transcription pathways that may down-modulate immune signalling and promote the establishment of chronic HCV infection.

MATERIALS AND METHODS

Cell Culture
Cell lines 293T, Huh7 and TZM-bl were cultured in DMEM. All media was supplemented with 10% heat inactivated FBS (non-US origin, Sigma-Aldrich) and 1% L-glutamine (Gibco) and cells grown at 5% CO_2/37°C. Similarly, J-Lat 10.6 cells were maintained in RPMI-1640 supplemented with 10% heat inactivated FBS (non-US origin, Sigma-Aldrich) and grown at 5% CO_2/37°C.

Cell Viability Assays
For measurement of cell viability following transfection with shRNA and viral envelope expression plasmids, 293T cells were seeded in a 12 well plate (7.5×10^4 per well). At 24 h post seeding cells were transfected with 150 ng of ATF3 shRNA plasmids or the scrambled shRNA or 12 ng of HCV E1E2, HCV SE2, HIV-1 JRFL (R5), HIV-1 LAI (X4), EBOV Env expressed plasmids using the polyethyleneimine (PEI) protocol. At 73 h post transfection cells were washed with PBS and 1:1 mixture of the cell suspension and 0.4% trypan blue solution was prepared. Cell viability was determined using automated cell counter. Similarly, viable cell counts for 293T and TZM-bl cells stably transfected with E1E2 were measured *via* 0.4% trypan blue solution and compared with the non-transfected cells.

Plasmid Preparation
Heat shock transformation followed by purification with Qiagen miniprep or maxiprep kits were used. In short, 2 μL plasmid stock (varying from 10 to 100 ng) was added to One Shot Top10 bacteria (ThermoFisher), mixed and incubated on ice for 30 min then incubated at 42°C for 30 s followed by 30 s on ice. 0.5 mL Super Optimal broth with Catabolite repression (SOC) media (ThermoFisher) was added and incubated for 1 h at 37°C with 180 rpm shaking before being plated on antibiotic selective agar plates overnight. Colonies were picked and grown in 5 mL Brain Heart Infuction (BHI)/ampicillin (100 μg/ml) culture (6 h - 16 h, 180 rpm at 37°C) for miniprep isolation (Qiagen), which was used to check plasmids before larger maxipreps were performed. For maxipreps (Qiagen), 250 mL BHI/ampicillin cultures were used and grown overnight using the same conditions as stated above.

Generation of Pseudo-Typed Viral Particles
HIV-1 JRFL (R5), HIV-1 LAI (X4), EBOV GP (Ebola) and HCV E1E2 Env (H77 isolate genotype 1a) were transfected into 293T cells in 10 cm dishes using the PEI protocol. For all transfections, PEI was diluted to 0.08 μg/μl in OptiMEM (Gibco) and all cells were incubated in 5% CO_2/37°C. For pseudo-typed virus particle production, the ΔEnv backbone pNL4-3-luc was used at 2,000 ng per condition as well as either 2000 ng of the HIV-1 Env expression plasmid, 285 ng of the Ebola Env plasmid or 200 ng of HCV Env E1E2 expression plasmids. In all cases, plasmids were added to 300 μl of Opti-MEM and this was then added to 300 μl of diluted PEI solution, mixed and incubated at rt for

20 min. Media was removed from 10 cm dishes and replaced with 1 ml Opti-MEM, and following incubation, transfection mix was added to cells dropwise and mixed and incubated under cell culture conditions for 6 h. Following this incubation, transfection media was replaced with DMEM.

Infection with Pseudo-Typed Viral Particles

Infections were performed on TZM-bl, Huh7 and 293T cell lines. Viral stocks were quantified *via* capsid-p24 standardised input. Target cells were seeded in 96 well plates (1.5×10^4 cells/well) 24 h prior to infection. Media was removed from the plate before 50 µL required media was added, followed by 100 µL of virus stock. After 6 h of incubation an additional 100 µL of appropriate cell media was added to each well and 48 h later cells were lysed and luciferase activity was quantified using BMG Labtech FLUOstar Omega with 100 µl luciferase substrate (Promega) injected per well.

Viral Quantification (p24 Capsid Assay)

The p24 assay was performed using recombinant p24 standard, p24 coating antibody (polyclonal sheep anti-HIV-1 p24 gag), secondary conjugate (alkaline phosphatase conjugate of mouse monoclonal anti-HIV-1 p24) from Aalto Bio Reagents Ltd and according to their protocol. Detection was performed using ELISA-Light Immunoassay System with CSP and Sapphire-I Substrate/Enhancer (ThermoFisher). All samples were diluted using 0.1% Empigen/TBS. Luminescence from ELISA plates was measured using a BMG Labtech FLUOstar Omega luminometer with a reading interval of 1 sec/well.

LTR, sE2 and E1E2 Transfection of Cell Lines

293T cells were seeded on 96 well plates (1.5×10^4 cells/well). When confluent, media was removed and 50 µL of Opti-MEM added to each well. Two µL Opti-MEM added per well with the following plasmid quantities: 12, 6 or 1 ng E1E2 or sE2 plasmid (nanogram quantity equalised with pCDNA between conditions), 6 ng LTR and 1 ng Tat. PEI was diluted to 0.14 µg/µl in 200 µL Opti-MEM and 2 µL of the diluted PEI was added to the plasmid mix. The plasmid/PEI mix was incubated at rt for 30 min before being added to cells and incubating for 6 h at 5% CO_2/37°C after which Opti-MEM/plasmid mix was removed and 250 µL DMEM added. Plates were measured for luciferase activity 48 h after transfection as described above. The following genotypes of HCV E1E2 Env were used – 1a, 1b, 2b, 3, 4, 5 and 6 (44, 45). HCV sE2 plasmids containing the gene fragment for the soluble ectodomain of the HCV E2 protein (aa363-661, referenced to the HCV strain H77 polyprotein) were PCR amplified from full length E1/E2 plasmids using genotype-specific primers [primer sequences described previously (45)] and Expand High-Fidelity Polymerase PCR System (Roche). PCR products were sub-cloned into the pCDNA plasmid and possessed an in-frame C-terminal 6xHis tag sequence. The following genotypes of HCV sE2 envelope were used – 1a, 1b, 2b, 4, 5 and 6. No corresponding sE2 genotype 3a plasmid was available.

Western Blot Analysis

Activating Transcription Factor 3 (ATF3) protein expression was determined in 293T cells transfected with ATF3 shRNA expression plasmids, HCV E1E2 Env and scrambled shRNA and pCDNA controls using western blot. Following transfection, cells were washed in ice cold dPBS and lysed with radioimmunoprecipitation assays (RIPA) buffer that included a 1% protease inhibitor cocktail (Thermo Scientific) and the protein concentration was subsequently quantified by the Bradford assay using the Protein Assay kit (Bio-Rad). 30 µg of cell lysates were mixed with 4x NuPage LDS Sample Buffer and 10x NuPage reducing agent, incubated at 72°C for 10 mins and loaded onto polyacrylamide gels (NuPAGE 12% Bis-Tris Gels; ThermoFisher), and electrophoresed at 120 V for 60 min.

Separated proteins were transferred to iBlot[TM] 2 PVDF Mini Stacks membranes (ThermoFisher) employing the iBlot 2 Dry Blotting system. The membranes were then blocked using the iBind solution kit (ThermoFisher) and incubated with primary and secondary antibodies using the iBind device (Invitrogen, USA) for 3 h. Antibodies used in this study included rabbit anti-ATF3 (1:250, Abcam), rabbit anti-β-actin (1:250, Abcam) and horseradish peroxidase (HRP) conjugated secondary antibody (anti-rabbit IgG; 1:1000; Bio-Rad). Protein bands were visualized using Pierce[TM] ECL Plus Western Blotting Substrate (ThermoFisher).

Stable Cell Line Production

TZM-bl cells were seeded in a 12 well plate (7.5×10^4 cells/well). At 24 h post seeding cells were transfected with either an E1E2 or sE2 expression plasmid containing a V5 tagged genotype 1A E1E2 or sE2 gene (expressing neomycin resistance) using the PEI protocol. Briefly, the transfection mix was prepared by diluting PEI to 0.08 µg/µl in 50 µL Opti-MEM to which 50 ng of envelope plasmid was added. This mix was incubated for 30 min at rt before being added to the well and incubated for 6 h in cell culture conditions, after which Opti-MEM/plasmid mix was removed and 1 mL DMEM was added. At 48 h post transfection media was refreshed using antibiotic selection (optimised as 400 µg/ml G418). Resistant cells were expanded before being tested for plasmid expression *via* FACS analysis (V5 directed Ab) and monitored periodically. TZM-bl-E1E2 and TZM-bl-sE2 cell lines were generated (E1E2: UKN1A20.8 EU155192. sE2: soluble E2_661 1A20.8.4). E1E2 and sE2 expression was confirmed *via* FACS staining of cells. In short, 2.5×10^5 cells were harvested 48 hours post transfection and were resuspended in 100 µl 4% paraformaldehyde solution for 20 minutes at 4°C. Cells were then washed twice in staining buffer (0.2 µm pore filtered PBS/1% heat inactivated FBS) and resuspended in fixation buffer (PBS/1% heat inactivated FBS/ 0.5% saponin) for 15 mins at room temperature. Cells were then resuspended in 50 µl fixation buffer containing the primary antibody (AP33 primary antibody at a 1:10 dilution) for 30 minutes at 4°C in the dark. Cells were washed with fixation buffer twice before being resuspended in 20 µl fixation buffer containing the secondary antibody (anti-mouse goat PE conjugate - 1:5 dilution), for 30 mins at 4°C in the dark. Cells were then washed

and resuspended in 200 µl staining buffer at 4°C in the dark until FACS analysis. The AP33 antibody recognises E2 epitopes between aa412-423.

Nuclear Extraction

TZM-bl and TZM-bl-E1E2 cells were grown to required confluency prior to extraction. Cells were washed with 10 mL cold PBS, followed by 10 mL cold PBS supplemented with 5 mM NaF and 1 mM Na_2MoO_4. 10 mL HB 1 x (2x: PBS supplemented with 40 mM HEPES, 10 mM NaF, 2 mM Na_2MoO_4 and 0.2 mM EDTA) was then added for 5 mins before being removed and 0.6 mL lysis buffer (10 mL HB 2x supplemented with 400 µL 10% NP-40 and 9.6 mL H_2O) added for a further 5 min incubation. The cells were transferred to an Eppendorf microcentrifuge tube and centrifuged at 13,000 rpm for 60 s. The supernatant was removed and the pellet resuspended in 50 µL resuspension buffer (10 mL HB 2x, 4 mL 97% glycerol and 6 mL H_2O). 60 µL salt buffer (10 mL HB 2x, 4 mL 87% glycerol, 4 mL 4M NaCl and 2 mL H_2O) was then added before the samples were incubated for 1 hr on a rotating wheel. 1 mL each resuspension buffer and salt buffer, supplemented with 40 µL PIC 25x (protease inhibitor cocktail, Sigma-Aldrich) and 100 µL Phospho Stop 10x (phosphatase inhibitor cocktail, Sigma-Aldrich) added prior to use. The samples were centrifuged at 13,000 rpm for 10 min before protein concentration quantified *via* the Bradford assay. Once quantified, the samples were aliquoted and stored at -80°C. All steps of this protocol were undertaken either on ice or at 4°C. Bradford quantification was performed using Quick Start Bradford Reagent (Bio-Rad).

HIV-1-LTR Capture Probe Synthesis and Affinity Purification

The DNA capture probe production and affinity purification were performed as described (46). Briefly, 20 pmoles of a 226-bp-long desthiobiotinylated double-stranded oligonucleotide corresponding to a fragment of the HIV-1 5' LTR (nt 229–455, where nt 1 is the start of the 5' LTR U3 region) that contains 2 NF-κB binding sites was produced by polymerase chain reaction (PCR) and immobilized on 1 mg of streptavidin-coated magnetic beads. 1 mg of protein nuclear extract prepared as described above was incubated for 2 h with the DNA-coated beads. After washes, biotin was used to specifically elute the protein-DNA complexes, before protein digestion with trypsin. Excess of biotin was finally removed by an additional incubation in the presence of 600 µg of fresh streptavidin-coated magnetic beads.

Liquid Chromatography/Tandem Mass Spectrometry Analysis and Protein Identification

Peptides were analysed using nano-LC-ESI-MS/MS maXis Impact UHR-TOF (Bruker, Bremen, Germany) coupled with a UPLC Dionex UltiMate 3000 (ThermoFisher). Digests were separated by reverse-phase liquid chromatography using a 75 µm X 250 mm reverse phase column (Acclaim PepMap 100 C18, ThermoFisher) in an Ultimate 3000 liquid chromatography system. Mobile phase A was 95% of 0.1% formic acid in water

and 5% acetonitrile. Mobile phase B was 0.1% formic acid in acetonitrile. The runtime was 120 min. The digest (15 µL) was injected, and the organic content of the mobile phase was increased linearly from 4% B to 35% in 90 min and from 35% B to 90% B in 5 min. The column effluent was connected to a Captive Spray (Bruker). In survey scan, MS spectra were acquired for 0.5 s in the m/z range between 50 and 2200. The 10 most intense peptides ions 2+ or 3+ were sequenced. The collision-induced dissociation (CID) energy was automatically set according to mass to charge (m/z) ratio and charge state of the precursor ion. The MaXis and the Ultimate systems were piloted by Compass HyStar 3.2 (Bruker).

Peak lists were created using DataAnalysis 4.1 (Bruker) and saved as MGF file for use with ProteinScape 3.1 (Bruker) with Mascot 2.4 as search engine (Matrix Science). Enzyme specificity was set to trypsin, and the maximum number of missed cleavages per peptide was set at one. Carbamidomethylation was allowed as fixed modification, oxidation of methionine, Gln–pyro-Glu and Carbamidomethylation (N-term) were allowed as variable modification. Mass tolerance for monoisotopic peptide window was 7 ppm and MS/MS tolerance window was set to 0.05Da. The peak lists were searched against a subset from the taxonomy homo sapiens of the UNIPROT database (162267 entries). Scaffold software (Scaffold 4.8.4, Proteome Software) was used to validate MS/MS based peptide and protein identification. For each sample, two analyses were made and results coming from Mascot were merged before performing a second search with X! Tandem (The GPM, the gpm.org). Peptide identifications were accepted if above 75% probability to achieve an FDR less than 1% by the Scaffold local FDR algorithm. Protein identifications were accepted if above 11% probability to achieve an FDR less than 2% and contained at least 2 identified peptides. Proteins sharing significance peptide evidence were grouped into clusters. Spectral counting quantitative analysis was used to compare the samples. T-test with a significance level of $p<0.05$ and a normalization based on total spectra were applied to the results.

Gene Expression PCR Detection

293T cells were plated o/n in six well plates ($2.5x10^5$ cells per well). The media was replaced with 500 µL of Opti-MEM per well. 250 ng DNA was added to 300 µL Opti-MEM media and mixed with 300 µL 0.08 µg/µl PEI and incubated for 30 mins before added to the cells and incubated for 48 h. Total RNA was extracted using the RNeasy Mini Kit (Qiagen). Reverse transcription of total RNA was performed using the Superscript III cDNA kit (ThermoFisher). Quantitative RT-PCR measuring relative expression of NF-κB (SinoBilogical, HP 100039), RELA (SinoBilogical, HP100270), IFI16 (ThermoFisher, Hs06603201_cn) and RBMX (ThermoFisher, Hs02426405_cn) was performed using SYBR green master mix, 1 µL primers, 4 µL nuclease free water and 5 µL of cDNA in total reaction volume of 20 µL. GAPDH (SinoBilogical, HP100003) was used as a control housekeeping gene. Samples were amplified and detected using a GeneRoter (Qiagen). Reactions were prepared in triplicate for each sample. PCR reaction conditions: 50°C for 2 min, 95°C for 5 min, 95°C for 10 s, 60°C for 20 s, 72°C for 10 s and a total of 40 amplification cycles

were performed with the final extension being 60°C for 5 min. The results were normalised to GAPDH expression.

MinION RNA-Seq

293T cells were seeded at 4.8×10^5 cells per well in a 6-well plate in 3.5 ml DMEM complete medium 24 h prior to transfection. On the day of transfection, culture medium was removed and replaced with 500 μl Opti-MEM. Transfection mix was prepared by diluting PEI to 0.08 μg/μl in 300 μl OptiMEM, to which 384 ng of HCV E1E2 glycoprotein expressing plasmid or control empty pCDNA vector was added and incubated at rt for 30 min. Transfection mix was added dropwise onto cells and incubated for 6 h in cell culture conditions. Following incubation, transfection mix was removed and replaced with 3.5 ml DMEM complete medium and incubated for 48 h. Cells were then washed in warm PBS and lysed using RLT lysis buffer (Qiagen) supplemented with β-mercaptoehtanol. RNA was purified from lysates using RNeasy Plus Minikit (Qiagen), according to manufacturer's instructions and eluted in 35 μl nuclease free water. RNA quality and purity were assessed using a Nanodrop spectrophotometer and Agilent Bioanalyzer, which indicated that all samples had an RNA Integrity Number (RIN) >9.3 (min 9.4 and max 10.0). RNA was quantified using Qubit high sensitivity RNA fluorometer. PolyA+ mRNA was purified from 35 μg total RNA using Dynabeads mRNA purification kit (ThermoFisher) and eluted in 15 μl of nuclease free water. Libraries were prepared using 30 ng polyA+ mRNA according to the Oxford Nanopore SQK-PCS-109 protocol in conjunction with EXP-PBC-001 barcoding kit to allow multiplexing of flow cells. Briefly, reverse transcription was performed using Maxima H Minus Reverse Transcriptase (42°C for 90 min, 85°C for 5 min) and 5 μl of reverse transcription product was separated into 2x 50 μl reactions with Oxford Nanopore barcoded primers for amplification (95°C for 5 min and 12 cycles of 95°C for 15 sec, 62°C for 15 sec and 65°C for 8 min, with final elongation at 65°C for 8 min). Amplification products were pooled and purified using Ampure XP magnetic beads (Beckman Coulter) with a 0.45x ratio of beads to DNA volume. Three adapted libraries were sequenced per flow cell, using 100 ng of each library. Libraries derived from control pCDNA transfected cells and libraries derived from HCV E1E2 transfected cells were sequenced on the same flow cells to limit flow cell associated bias. Sequencing was performed using MIN-106 flow cells (R9.4.1 or R9.4 pores) on the Oxford Nanopore MinION sequencing platform. Run durations ranged from 12-24 h.

Differential Gene Expression Analysis

MinION reads were basecalled using Oxford Nanpore's Guppy Basecaller software (version 3.2.4) and reads with a q-score <7 were discarded during basecalling. Each sequencing library was demultiplexed and adapter sequences were trimmed using Porechop (https://github.com/rrwick/Porechop). To confirm expression of HCV E1E2 in transfected cells, libraries were mapped to a database of viral genomes using Kraken2 (47). Reads were then mapped to human genome HG38 (GCA_000001405.15) using Minimap2 (48) with parameters "–ax –splice -k14". Mapped reads were assigned to genomic features using featureCounts (49).

Normalisation of raw read counts was performed using the EdgeR "trimmed mean M-values (TMM)" method (50). Genes with read counts lower than a sufficient value were filtered out using the EdgeR function "filterByExpr" with the default parameters (50). Differential gene expression between E1E2 or pCDNA transfected cells was determined using the R package Limma, using the "voom" method with a cut off of p=0.05 (51, 52). clusterProfiler was used to determine the biological themes of differentially expressed genes (53). Gene set enrichment analysis was performed with 10,000 gene set permutations to identify possible pathways that may be affected by E1E2 (54).

ATF3 shRNA Knock-Down

Three ATF3 directed shRNA and a scrambled expression plasmid (pSUPER) were a kind gift from Dr Martin Janz (Max Delbrueck Center for Molecular Medicine and Charité, University Hospital Berlin) (55). 293T cells were seeded in 24 well plates (1×10^5 cells per well) 24 h prior to transfection. On day of transfection, medium was replaced with 100 μl Opti-MEM. Transfection mix was prepared by diluting PEI to 0.08 μg/μl in 50 μl Opti-MEM to which 300 ng of ATF3 shRNA plasmids or the scrambled shRNA or pCDNA control was added. The mix was incubated at rt for 30 min before adding to cells and incubated for 6 h after which the Opti-MEM/plasmid mix was removed and 1 ml DMEM added. After 48 h cells were re-transfected with 50 ng of LTR-Luc and 5 ng Tat expression plasmids, using the same conditions as described above. The plate was measured for luciferase activity 48 h after transfection. Similar was performed utilising a 96 well plate format (1.5×10^4 cells per well) following the same procedures with reagent volumes and quantities adjusted accordingly.

Statistical Analysis

Statistical analysis was performed using GraphPad Prism 8 software unless specified otherwise. For RNAseq, statistical analysis was performed using R packages Voom/Limma. Data were analysed using the Kruskal-Wallis one-way analysis of variance followed by using Dunn's analysis to perform paired multiple comparisons. Ns – non-statistical. * P<0.05. ** P<0.01.

RESULTS

HCV E1E2 Env Glycoprotein Down-Modulates HIV-1 Viral Production

Pseudo-typed lentiviral particle systems are routinely utilised to study viral phenotypes (including HIV-1, HCV, Ebola virus and coronavisuses). Transfection of 293T producer cells with a plasmid expressing the HIV-1 viral backbone minus the Env gene (Δenv) in conjunction with a plasmid expressing viral Env proteins was performed. When producing pseudo-typed lentiviral particles expressing the HCV envelope E1E2 a virus stock was generated that infects liver derived Huh7 cells but not TZM-bl cells, indicating HCV E1E2 protein expression (**Figure 1A**). Through generating pseudo-typed viral stocks expressing variant Env proteins [HIV-1 (R5), HIV-1 (X4), HCV Env and Ebola virus glycoprotein (GP)] a consistent decrease in viral p24 production was observed for the HCV E1E2 stocks in comparison to other viruses (observed in >3

FIGURE 1 | The HCV E1E2 Env and sE2 Env proteins can restrict HIV-1 replication, reduce HIV-1 infectious virus production and restrict proviral activation. **(A)** Pseudo-typed virus and infection of TZM-bl or Huh7 cell lines. ΔEnv backbone, JR-FL HIV-1 (CCR5 using) Env pseudo-typed virus, LAI HIV-1 Env (CXCR4 using) pseudo-typed virus, E1E2 HCV Env pseudo-typed virus and Ebola virus (EBOV) Env GP pseudo-typed viruses were infected onto TZM-bl and Huh7 cells using a standardised 10 ng (p24) of pseudo-typed virus input. Infection was quantified *via* luciferase readout (RLUs) (n=3). **(B)** Pseudo-typed virus quantification *via* p24 capsid ELISA (ng/mL) for each of the enveloped viruses with ΔEnv virus used as a control (n=2). **(C)** Replication curves of LAI-YFP (TCID50/ml 10,000 infectious titre) on three cell lines: TZM-bl, TZM-bl-E1E2 and TZM-bl-sE2. Replication was quantified *via* p24 capsid ELISA at four timepoints: day 4, 7, 10 and 14 post infection (n = 4). **(D)** The production of virus as quantified *via* p24 capsid ELISA at day 7 from J-Lat 10.6 cells post TNFα activation and transfection of cells with Env glycoproteins or pCDNA empty vector (n = 4). Kruskal-Wallis and Dunn's test were used to analyse significance between the control cells and all other conditions. *P < 0.05. For all graphs mean is plotted and error bars represent standard deviation.

different experiments) (**Figure 1B**). We confirmed HCV E1E2 Env expression from analysing stably transfected TZM-bl cells with a plasmid expressing a tagged E1E2 molecule using FACS (**Supplementary Figure 1**). These findings identify that expression of the HCV E1E2 Env protein down-modulates pseudo-typed viral production in 293T producer cells.

HCV E1E2 and sE2 Expression Can Reduce HIV-1 Replication and Activation

From the above observations, we hypothesised that specific expression of HCV E1E2 protein can down-modulate HIV-1 production and/or viral replication. To test this, we generated TZM-bl cell lines that transiently express either HCV Env E1E2 or the soluble E2 (sE2) protein under drug selection (TZM-bl-E1E2 and TZM-bl-sE2, respectively). Plasmids were generated which expressed HCV E1E2 or sE2 carrying a V5 tagged epitope which allowed for testing transfected cell lines and confirming protein expression (**Supplementary Figure 1**). HIV-1 replication was monitored on TZM-bl, TZM-bl-E1E2 and TZM-bl-sE2 cell lines using replication competent LAI-YFP virus (1×10^3 TCID$_{50}$/ml input) and sampling viral p24 production (**Figure 1C**). Viral replication was highest on TZM-bl cells with a delay in viral

replication observed on TZM-bl-sE2 cells, whereas replication was suppressed on TZM-bl-E1E2 cells (**Figure 1C**).

We next investigated the effects of HCV Env glycoprotein expression on suppressing HIV-1 activation in a cell line used as a model of HIV-1 viral latency (J-Lat-10.6). This cell carries a single integrated HIV-1 genome that can be activated with Tumour Necrosis Factor α (TNFα). An array of plasmid constructs (pCDNA, E1E2 and sE2) were transfected into J-Lat-10.6 cells, which were subsequently activated with TNFα and monitored for viral p24 production (**Figure 1D**). In the absence of TNFα activation, expression of viral p24 from J-Lat 10.6 was measured over several experiments and was consistently below the limit of ELISA detection (data not shown). Expression of both HCV E1E2 and sE2 suppressed induction of viral activation (P<0.05) in comparison to pCDNA.

HCV Glycoproteins Repress HIV-1 TR Activity

The above indicated that the HCV E1E2 Env protein has the capacity to reduce HIV-1 activity. We next tested the effects of increasing concentrations of different Env proteins on modulating viral production and demonstrated that higher concentrations of E1E2 transfection limited viral production (P<0.01) (**Figure 2A**), which was not observed for either HIV-1 Env (JR-FL) or Ebola virus GP (**Figures 2B, C**, respectively). In order to examine this HCV dependent effect on modulating LTR activity, different concentrations of E1E2 or sE2 were co-transfected along with a plasmid containing the luciferase (Luc) gene under the control of an HIV-1 LTR promotor (HIV-1 subtype B) into 293T cells (**Figures 2D, E**, respectively). Additionally, the HIV-1 Tat protein was co-transfected with the LTR plasmids to enhance LTR activation, which was quantified by measuring luciferase activity in transfected cell lysate. Inhibition was observed with both increasing concentrations of E1E2 (P<0.05) (**Figure 2D**) and sE2 (P<0.05) (**Figure 2E**), with sE2 showing a stronger inhibitory effect. In addition, we tested the homologous non-primate hepacivirus (NPHV) E1E2 protein for down-modulation of HIV-1 LTR activity and found a similar dose dependent decrease in LTR activation (P<0.05) (**Figure 2F**). Further, to ensure that the observed down-modulation was not due to toxicity of transfection or expression of the envelopes themselves, cell viability following transfection with various envelopes was measured (**Supplementary Figure 5D**). This indicated that viral Env proteins with sufficient homology to the HCV E1E2 protein can repress HIV-1 LTR activity.

Due to the E1E2 and sE2 effects observed above, we aimed to determine whether E1E2 derived from different HCV genotypes could similarly affect the activity of multiple HIV-1 LTR subtypes. Differences are present in the number and type of transcription factor binding sites present within the HIV-1 LTR as shown (**Figure 3**). Therefore, to evaluate the effect of HCV Env E1E2 on HIV-1 LTR activity, a Tat expressing plasmid as well as a panel of plasmids containing HIV-1 variant subtype specific LTRs cloned upstream of a reporter Luc gene were transfected into TZM-bl and TZM-bl-E1E2 cells. LTR activity was quantified *via* luciferase activity and there was a generalised E1E2 mediated down-
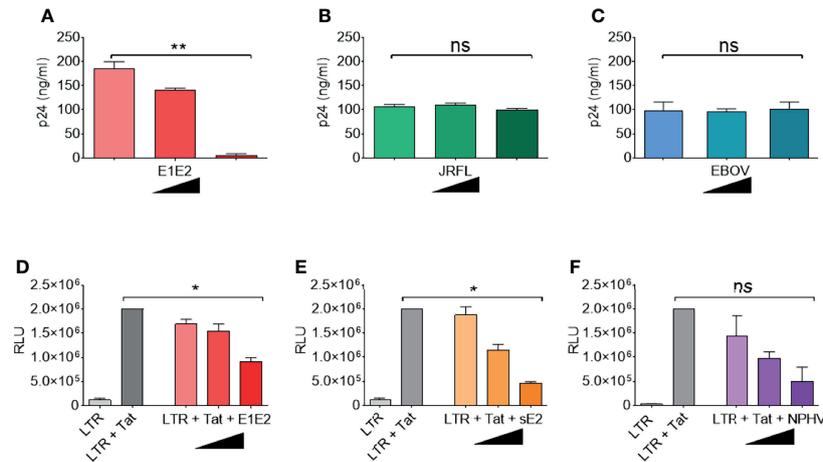
FIGURE 2 | HCV E1E2 and sE2 Env proteins down-modulate HIV-1 LTR activity. **(A–C)** the p24 ng/ml quantification of virus generated by transfection of ΔEnv HIV-1 plasmid in conjunction with with increasing concentrations (9 ng, 90 ng and 900 ng) of the following: **(A)** HCV E1E2 Env expression plasmid (n = 4), **(B)** the HIV-1 JR-FL Env expression plasmid and (n = 4) **(C)** Ebola virus GP Env expression plasmid (n = 4). **(D–F)** LTR activation in 293T cells as quantified by luciferase when 6 ng LTR was co-transfected with HIV-1 1 ng Tat expression plasmid and in conjunction with different concentrations of **(D)** HCV E1E2 Env expression plasmid (n = 4) **(E)** HCV sE2 Env expression plasmid and (n = 4) **(F)** NPHV Env expression plasmid at three different concentrations for each (n = 4). Kruskal-Wallis and Dunn's test were used to analyse significance. *P < 0.05, **P < 0.01 and ns – not significant. For all graphs, mean is plotted and error bars represent standard deviation and black triangles are used to depict increasing concentrations of plasmid (from 1 ng, to 6 ng and to 12 ng).

modulation of LTR activity across all HIV-1 subtype-specific LTRs tested (LTRs A, B, C, D, E, F and G) (**Figure 4A**). Additionally, to ensure that down-modulation of LTR activity was not due to toxicity of E1E2 expression or of transfection of LTR subtypes, viable cell counts were compared between TZM-bl and TZM-bl-E1E2 cells (**Supplementary Figure 5B**) as well as between 293T and 293T-E1E2 cells (**Supplementary Figure 5A**) transfected with various LTR subtypes.

We next sought to determine the effects of individual HCV E1E2 or sE2 Env genotypes (1a, 1b, 2b, 3, 4, 5, 6) against three selected HIV-1 LTR promoter subtypes (A, B and E). Two concentrations of E1E2 or sE2 plasmids (12ng and 1ng) were co-transfected along with the LTR plasmids in conjunction with the Tat expressing plasmid. Transfection of LTR subtype A with E1E2 demonstrates the ability of E1E2 to down-modulate LTR activation (**Figure 4B**), with the higher concentration showing more inhibition. When testing LTR subtype B, there is again a generalised down-modulation of LTR activity with the higher concentration of E1E2 Env plasmid (**Figure 4B**). With the subtype E LTR construct, a higher frequency of E1E2 genotypes did not demonstrate dose-dependent down-modulation of LTR expression (2b, 4 and 5) whereas other genotypes did and in general, lower expression was observed with sE2 for all genotypes (**Figure 4B**). When transfecting HIV-1 LTR A in conjunction with the sE2 expressing plasmid, a greater effect on LTR down-modulation was observed in comparison to E1E2 (**Figure 4C**). With regards to LTR B, the differences between LTR activation profiles with sE2 (**Figure 4C**) was shown to be greater than with E1E2 (**Figure 4C**). For example, there is a 6-fold difference in LTR activation between HCV Env genotype 4 with sE2 expression (12ng and 1ng) in comparison to a 3-fold difference with genotype

4 with E1E2. In addition, with genotype 5 and sE2 there was a 7-fold difference between 12 and 1ng in comparison to the smaller and relatively similar decrease with regards to genotype 5 and E1E2 Env. Similarly, when LTR E was transfected with sE2, as with LTR B, genotype 5 showed a greater effect than when transfected with E1E2 (**Figure 4C**). It should be noted that LTR E contains only one NF-κB binding site as opposed to the two found in subtypes A and B, and that the down-modulatory effect of E1E2/sE2 remains consistent (**Figures 4B, C**). Whilst statistical significance in relation to down-modulation of LTR activity is not observed across all conditions, the same trend is observed, indicating a generalised effect of E1E2 or sE2 on LTR activity irrespective of HCV genotype and where sE2 shows the greater down-modulation.

HCV Glycoproteins Repress HIV-1 LTR Activity *via* an NF-κB Dependent Process

To identify whether the effect on LTR activation is a result of E1E2 or sE2 protein and not an mRNA mediated effect, an HCV E1E2 genotype 6 knock-out (KO) mutant plasmid was generated and used to transfect 293T cells. It was observed that LTR activity was down-modulated in the presence of E1E2 protein (ATG+) (P<0.05) but not when E1E2 protein expression was knocked-out (ATG – KO Mut) (**Figure 5A**). Since the NF-κB pathway accounts for a significant proportion of LTR activation, this was chosen as a target for further investigation. To determine whether HCV glycoprotein mediated repression of HIV-1 LTR was most likely a result of affecting the NF-κB signalling pathway, a series of reporter plasmids were transfected into Huh7 cells or Huh7 cell lines stably expressing E1E2. Both NiFty-luc (5x NF-κB binding sites) and ConA (3x NF-κB
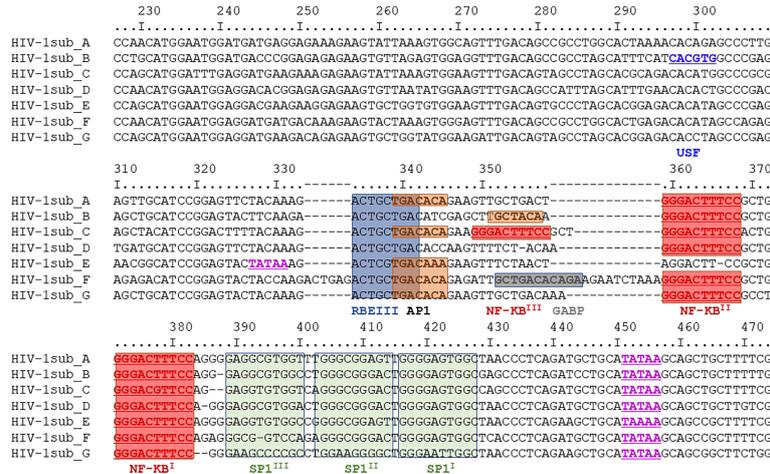
FIGURE 3 | Nucleotide sequence comparison of HIV-1 LTR subtypes A-G. The region depict covers nucleotides 229 – 455 and with transcription factor binding sites highlighted: USF sites in dark blue, TATAA sites in purple, RBEIII sites in light blue, AP1 sites in orange, NF-κB sites in red, GABP sites in dark grey and SP1 sites in green. This same region represents the DNA subtype B LTR pull-down probe described in section 3.5.

binding sites) are plasmids that express luciferase under the control of NF-κB dependent promoters and show a significant

FIGURE 4 | E1E2 and sE2 down modulates LTR activity of variant HIV-1 sub-types and by different HCV Env genotypes. **(A)** Transfection of LTR-luc plasmids into two cell lines: TZM-bl (grey) and TZM-bl-E1E2 (red) with 1 ng Tat plasmid also transfected in to activate the LTRs (n = 3). LTR activity was quantified *via* luciferase RLUs. **(B)** HIV-1 LTR-A, LTR-B and LTR-E activation when 293T cells co-transfected with two concentrations of E1E2 plasmid (12 ng represented by dark red bars, and 1 ng represented by light red bars) (n = 3) or **(C)** HIV-1 LTR-A, LTR-B and LTR-E activation when 293T cells co-transfected with two concentrations of sE2 plasmid (12 ng represented by dark orange bars, and 1 ng represented by light orange bars) (n = 3). For LTR control condition, 6 ng LTR-luc was transfected alone or in combination with 1 ng Tat expression plasmid. For all graphs, mean values are plotted and error bars represent standard deviation and statistical comparisons were performed utilising a Kruskal-Wallis and Dunn's test comparing the activity between the control LTR + Tat transfection and with variant concentrations of E1E2 or sE2. *P < 0.05. **P < 0.01.

decrease in luciferase activity in the presence of E1E2, by 28-fold (P<0.01) and 19-fold (P<0.01), respectively (**Figure 5B**). Conversely, ATX-luc and 90K-luc are plasmids that express luciferase under the control of general cellular promoters (autotaxin and 90K) and are not reliant on NF-κB and demonstrated no significant difference in luciferase activity in the presence of E1E2. Taken together, these results indicate that the previously observed E1E2 dependent reduction in LTR activity is a result of disruption to NF-κB signalling, which is protein (not RNA) dependent (**Figure 5C**).
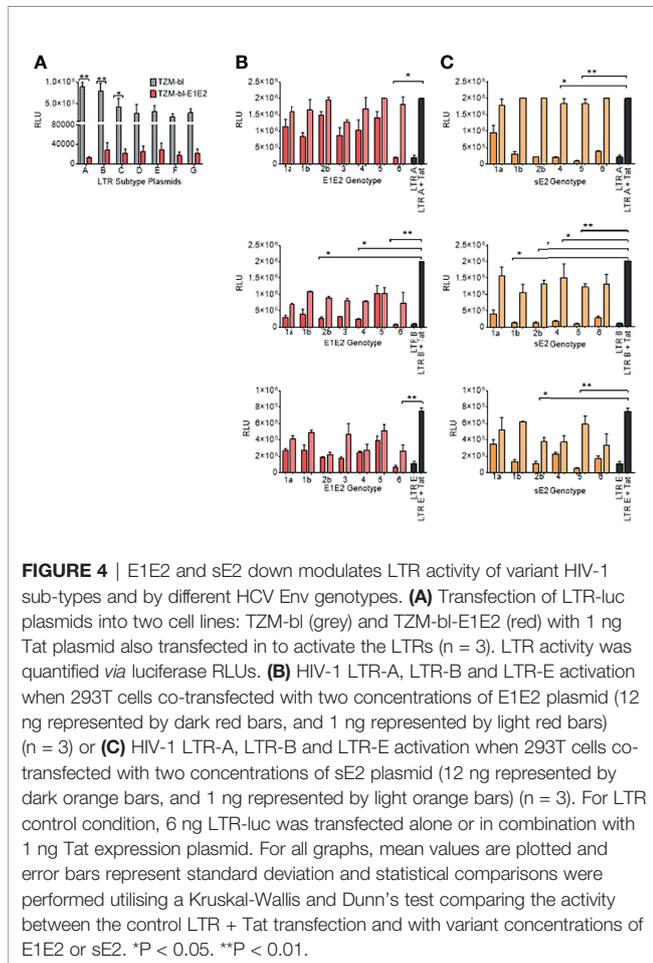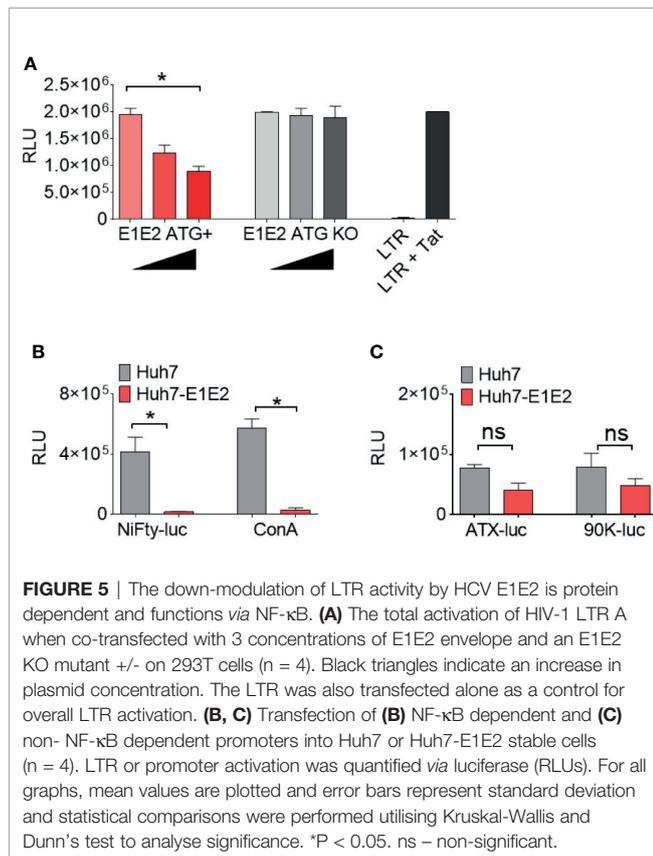
E1E2 Down-Modulation Associates with Disruption of Transcription Factors, Including NF-κB Binding to the HIV-1 LTR

The NF-κB signalling network is a diverse and complex series of pathways. As NF-κB dependent promoter activity was down-modulated by the presence of E1E2, we aimed to identify the mechanism by which this occurs. We analysed, in an unbiased fashion, the differential binding of proteins to the HIV-1 LTR in the absence or presence of the HCV E1E2 protein. The affinity purification followed by mass spectrometry (AP-MS) strategy utilises a double stranded LTR DNA capture probe to pull-down proteins from cells transfected with pCDNA control plasmid or with plasmid expressing HCV E1E2 (the natural Env protein being expressed in infected cells) and analysed the nuclear extract from these cells. The LTR probe was generated as a PCR template of WT HIV-1 5'LTR (subtype B, nucleotides 229 – 455) (covering the region as depict in **Figure 3**) before being incubated with nuclear extract generated from the two target cell lines (TZM-bl and TZM-bl-E1E2). The probe-protein complexes were treated with trypsin before analysis by reverse phase liquid chromatography and mass spectrometry to identify the probe-bound proteins (46). Gene ontology analysis with DAVID was performed on the 187 proteins confidently identified. The two most enriched processes were "Transcription" (64 proteins;

FIGURE 5 | The down-modulation of LTR activity by HCV E1E2 is protein dependent and functions *via* NF-κB. **(A)** The total activation of HIV-1 LTR A when co-transfected with 3 concentrations of E1E2 envelope and an E1E2 KO mutant +/- on 293T cells (n = 4). Black triangles indicate an increase in plasmid concentration. The LTR was also transfected alone as a control for overall LTR activation. **(B, C)** Transfection of **(B)** NF-κB dependent and **(C)** non- NF-κB dependent promoters into Huh7 or Huh7-E1E2 stable cells (n = 4). LTR or promoter activation was quantified *via* luciferase (RLUs). For all graphs, mean values are plotted and error bars represent standard deviation and statistical comparisons were performed utilising Kruskal-Wallis and Dunn's test to analyse significance. *P < 0.05. ns – non-significant.

p-value 5.1×10^{-18}) and "Transcription Regulation" (53 proteins; p-value 9.4×10^{-12}), based on normalized spectral count analysis of the data, a large number of proteins were found to differentiate in binding to the HIV-1 LTR, with 22 proteins binding in the presence of HCV E1E2 and 34 proteins enriched in the control experimental conditions (**Supplementary Table 1**). Detailed analysis of these 56 differentially bound proteins revealed that most of them possess DNA binding activity and/or transcription regulation properties, as indicated by the Uniprot database. In addition, all the proteins in italics in **Table 1** have been previously reported to play a role in HIV-1 replication (according to PubMed), consistent with the high quality and relevance of this data.

When comparing the proteins binding to HIV-1 LTR some clear differences were found (**Table 1**). The most interesting findings being that several positive transcriptional regulators of HIV1-LTR transcription were found exclusively or more abundantly in the HIV-1 LTR pull-down performed in the absence of E1E2, suggesting that these positive regulators are inhibited by E1E2 expression. This concerns 3 members of the NF-κB family (NF-κB1, NF-κB2 and RelA), the Specificity Protein 1 (SP1), which was one of the very first positive regulator of HIV-1 transcription described (56), COUP TF, which stimulates HIV-1 transcription (57), in cooperation with Nuclear receptor subfamily 2 group C member 2 (NR2C2), also called thyroid receptor 4 orphan receptor (58). The same differential pull-down profile is observed for the DNA repair proteins XCCR5 and XCCR6

compose the Ku complex, described to bind directly to the HIV-1 LTR, promoting early transcription from the promoter (59). Unexpectedly, while the interferon gamma inducible protein 16 (IFI16) was exclusively found in the HIV-1 LTR pull-down in the absence of E1E2, this protein is described to target the SP1 positive transcription factor to suppress HIV-1 transcription (60). Amongst the proteins that bound to the LTR probe in the presence of E1E2, we found the non-POU domain-containing octamer-binding protein (NoNO), a transcription factor that negatively regulates HIV-1 infection in T lymphocytes (61), Helicase-like transcription factor (HLTF), that has been shown to restrict HIV-1 replication (62), PARP-1, a negative regulator of HIV-1 transcription (63) and replication (64) or RBMX which has recently been shown to bind the HIV-1 LTR proviral DNA to maintain the viral latency (65).

The differential binding profile of transcriptional regulators identified in the DNA pull-down is consistent with the data obtained with the HIV-1 LTR luciferase reporter and HIV-1 replication, since most negative regulators are found in the experimental condition where E1E2 is expressed, while the positive regulators are more abundant in the absence of E1E2. However, the mechanisms by which E1E2 induces this switch is currently not known. The results suggest a wide-range of alterations in transcription factors binding to the HIV-1 LTR associated with HCV E1E2 Env expression. We selected a number of the transcription factors associated with our findings (NF-κB p50, RelA, IFI16 and RBMX) to identify whether the protein binding alterations observed correlated to alterations at the mRNA expression levels. Quantification assays were developed for each gene, but no differences were found in mRNA expression for NF-κB, RelA, IFI16 or RBMX (**Supplementary Figures 2A–D**). These results demonstrate a scenario where the disruption to NF-κB binding the LTR is *via* post-transcriptional mechanism.

HCV Glycoproteins Activate Host Endoplasmic Reticulum Stress Pathways Known to Inhibit NF-κB Activity

We next measured differential gene expression (DGE) patterns between cells expressing the HCV E1E2 Env protein in comparison to cells transfected with the control vector, pCDNA (GEO accession: GSE163239). We selected to utilise the 293T cell line for differential gene expression analysis to provide consistency with results showing the effect of E1E2 expression on down-modulating HIV-1 LTR activity (section 3.2). Since the down-modulation of HIV-1 LTR activity in the presence of HCV E1E2 Env protein is similar between 293T and Huh7 cells we are confident our results are reflective of cell types infected with HCV. Initially, to demonstrate expression of E1E2, all the expression libraries were mapped to an HCV reference genome, highlighting expression of HCV derived genes only in the E1E2 transfected cells (**Figure 6A**). The effect of HCV glycoproteins on the cellular transcriptome was analysed using the Limma/Voom package following assessment of library length and quality distributions and sample clustering *via* principal component analysis (PCA) (**Supplementary Figures 3A-C**). Additionally, libraries were transformed and normalised using EdgeR,

TABLE 1 | Effect of the presence of E1E2 on the proteins captured by the HIV-1-LTR.

Protein name	Accession number	DNA binding	Transcript. regul.	E1E2	Control
Significantly enriched in control samples					
Nuclear factor NF-kappa-B p105 subunit	NFKB1_HUMAN	Y	Y	1	14
Nuclear factor NF-kappa-B p100 subunit	NFKB2_HUMAN	Y	Y	0	41
RELA protein	Q2TAM5_HUMAN	Y	Y	0	6
Cluster of Nuclear receptor subfamily 2 group C member 2	NR2C2_HUMAN	Y	Y	0	4
Cluster of COUP transcription factor 1	COT1_HUMAN	Y	Y	2	43
Cluster of X-ray repair cross-complementing protein 5	XRCC5_HUMAN	Y	Y	34	76
X-ray repair cross-complementing protein 6	XRCC6_HUMAN	Y	Y	61	118
Upstream stimulatory factor 1	USF1_HUMAN	Y	Y	0	7
Upstream stimulatory factor 2 (Fragment)	M0QXT0_HUMAN	Y	Y	0	10
Transcription factor Sp1	SP1_HUMAN	Y	Y	14	34
Cluster of Gamma-interferon-inducible protein 16	IFI16_HUMAN	Y	Y	0	132
Paired amphipathic helix protein Sin3a	SIN3A_HUMAN	/	Y	0	16
Cluster of Leucine-rich PPR-motif containing	E5KNY5_HUMAN	Y	/	0	5
Three prime repair exonuclease 1	Q5TZT0_HUMAN	Y	/	0	8
Cluster of Histone H2B type 1-C/E/F/G/I	H2B1C_HUMAN	Y	/	0	7
Cluster of Steroid hormone receptor ERR1	ERR1_HUMAN	Y	Y	0	8
DNA ligase 3	DNLI3_HUMAN	Y	/	0	22
Cluster of Histone H3	B2R4P9_HUMAN	Y	/	2	6
Cluster of Nuclear factor 1 A-type	NFIA_HUMAN	Y	Y	0	9
Cluster of Elongation factor 1-alpha 1	EF1A1_HUMAN	Y	/	2	18
DNA topoisomerase 2-alpha	TOP2A_HUMAN	Y	/	39	225
Cluster of DNA topoisomerase 2-beta	TOP2B_HUMAN	Y	/	22	265
Circadian locomoter output cycles protein kaput	CLOCK_HUMAN	Y	Y	0	11
Zinc finger BED domain-containing protein 6	ZBED6_HUMAN	Y	Y	0	13
Nuclear receptor V-erbA-related	F1D8R3_HUMAN	Y	Y	0	11
Cluster of Class E basic helix-loop-helix protein 40	BHE40_HUMAN	Y	Y	0	9
Cluster of DNA topoisomerase 1	TOP1_HUMAN	Y	/	8	55
Krueppel-like factor 13	KLF13_HUMAN	Y	Y	4	10
Cluster of Homeobox protein TGIF1	TGIF1_HUMAN	Y	Y	0	5
Mitochondrial DNA polymerase subunit gamma-2	E5KS22_HUMAN	Y	/	25	43
Endoplasmic reticulum chaperone BiP	BIP_HUMAN	/	/	0	13
Cluster of Epididymis secretory sperm binding protein Li 124m	V9HW84_HUMAN	/	/	1	10
p180/ribosome receptor	A7BI36_HUMAN	/	/	5	25
Cluster of Heat shock cognate 71 kDa protein	E9PKE3_HUMAN	/	/	9	29
Significantly enriched in E1E2 samples					
Helicase-like transcription factor	HLTF_HUMAN	Y	Y	54	4
Cluster of RNA-binding motif protein, X chromosome	RBMX_HUMAN	Y	Y	22	0
Cluster of Non-POU domain-containing octamer-binding protein	NONO_HUMAN	Y	Y	29	2
Poly [ADP-ribose] polymerase 1	PARP1_HUMAN	/	Y	768	388
Nucleolin	NUCL_HUMAN	Y	Y	19	2
Cluster of Lamina-associated polypeptide 2, isoform alpha	LAP2A_HUMAN	Y	Y	9	0
Cluster of cDNA FLJ54552, highly similar to Heterogeneous nuclear ribonucleoprotein K	B4DUQ1_HUMAN	Y	Y	86	33
Leucine-rich repeat and WD repeat-containing prot. 1	LRWD1_HUMAN	Y	/	4	0
Telomere-associated protein RIF1	RIF1_HUMAN	/	Y	20	1
Cluster of Heterogeneous nuclear ribonucleoprotein M	HNRPM_HUMAN	/	/	9	0
Acyl-CoA dehydrogenase family member 11	ACD11_HUMAN	/	/	26	0
Cytoskeleton-associated protein 5	CKAP5_HUMAN	/	/	28	0
Cluster of Glutamine–tRNA ligase	SYQ_HUMAN	/	/	12	0
Cluster of Epididymis luminal protein 189	Q5HYB6_HUMAN	/	/	31	1
cDNA, FLJ96156, highly similar to Homo sapiens leucyl-tRNA synthetase (LARS), mRNA	B2RCM2_HUMAN	/	/	14	0
Cluster of cDNA FLJ52761, highly similar to Actin, aortic smooth muscle	ACTBL2_HUMAN	/	/	279	32
Methionine–tRNA ligase, cytoplasmic	SYMC_HUMAN	/	/	5	0
Cluster of Myosin light polypeptide 6	MYL6B_HUMAN	/	/	42	0
Cluster of Myosin-10	MYH10_HUMAN	/	/	482	0
Cluster of Kelch-like protein 7	KLHL7_HUMAN	/	/	14	8
Myosin regulatory light chain MRCL3 variant (Fragment)	Q53HL1_HUMAN	/	/	23	0
Bifunctional glutamate/proline–tRNA ligase	SYEP_HUMAN	/	/	24	0

*Nuclear extracts proteins from TZM-bl cells transiently transfected with E1E2 plasmid ("E1E2") or with pCDNA plasmid ("control") were pulled-down with a HIV-1-LTR DNA fragment and identified by mass spectrometry. A quantitative analysis was performed to compare the normalized spectral count in E1E2 and control conditions, with a T-test comparison. Proteins with significant differences (p-value < 0.05) are shown, while all the results are presented in **Supplementary Table 1**. E1E2 S.C. and Control S.C. represent the merge of the normalized spectral counts of 3 biological independent replicates of the corresponding experimental condition. The mention of DNA-Binding and of Transcription Regulation activities was manually search in Uniprot database, and indicated by Y when present. The proteins reported to have a link with HIV (PubMed search) are indicated in italics. E1E2 S.C. and Control S.C. represent the merge of the normalized spectral counts of each replicate of the corresponding experimental condition.*

according to the method described (50–52) (**Supplementary Figures 3D, E**). Several genes were significantly upregulated in the presence of E1E2 when compared to control pCDNA transfected cells, and no genes were significantly downregulated (**Figure 6B**). In line with our previous experiments, we sought to determine the effect of E1E2 on the expression of cellular transcription factors such as NF-κB, that are known to interact with the HIV-1 LTR. In our dataset, expression of NF-κB, SP1, RelA and Jun were not significantly affected by the presence of E1E2 (**Figures 7A–D**).

The most significantly enriched biological processes are highlighted (**Figure 6C**), which shows that pathways involved in the endoplasmic reticulum (ER) stress response are enriched in the presence of E1E2 (**Figure 6C** and **Supplementary Figure 4**). Further, our analysis showed that the most significantly enriched pathways are all associated with ER stress or the cellular response to stress (**Supplementary Table 2** and **Supplementary Figures 4A–E**).
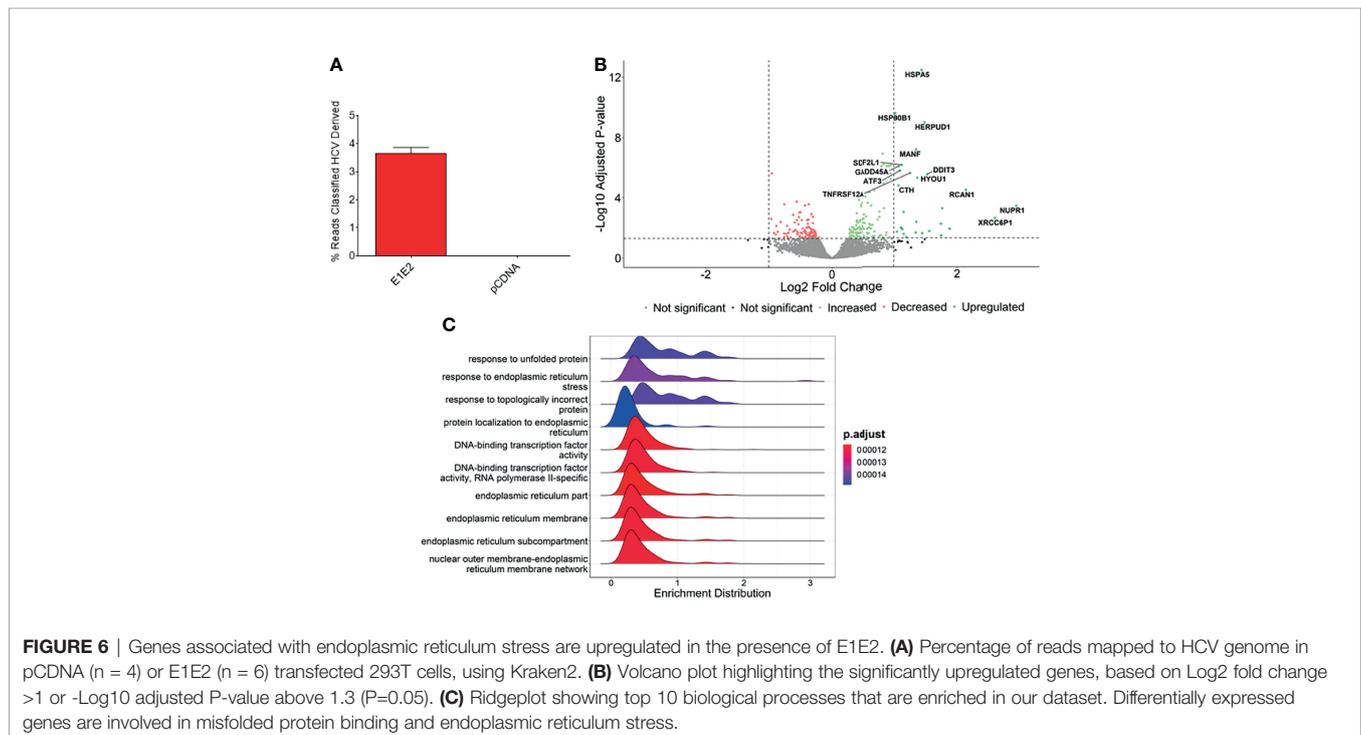
Individual genes that are significantly upregulated in our data set are associated with ER stress. Heat shock protein family A (Hsp70) member 5 (HSPA5) gene encodes the binding immunoglobulin protein (BiP) and is the most significantly upregulated gene in our dataset (**Figures 6B, 8A**). BiP is the master regulator of the UPR, and as such its overexpression indicates a cellular response to ER stress and explains the upregulation of other genes such as heat shock protein 90 beta family member 1 (HSP90B1) (**Figure 8B**), homocysteine inducible ER protein with ubiquitin like domain 1 (HERPUD1) (**Figure 8C**), stromal cell derived factor 2 like 1 (SDF2L1) (**Figure 8D**), activating transcription factor 3 (ATF3)
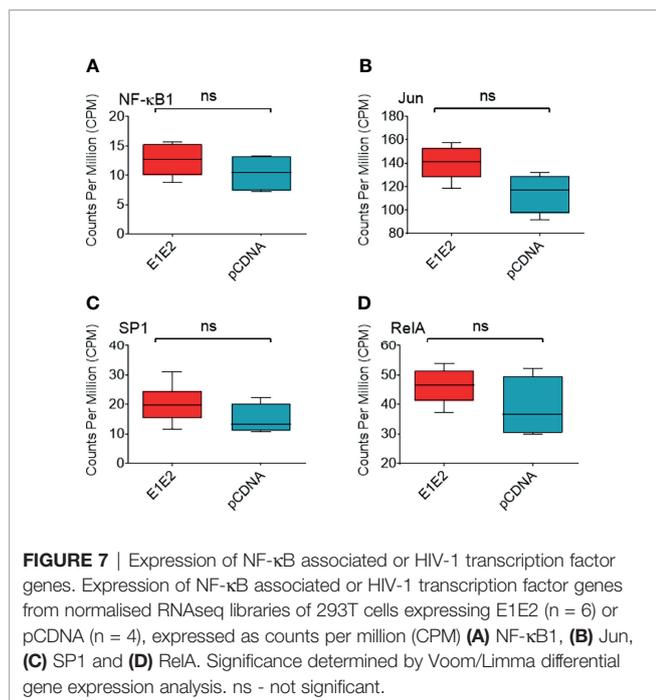
(**Figure 8E**), mesencephalic astrocyte derived neurotrophic factor (MANF) (**Figure 8F**), DNA damage inducible transcript 3 (DDIT3) (**Figure 8G**) and growth arrest and DNA damage inducible alpha (GADD45A) (**Figure 8H**). The upregulation of these genes strongly suggests that the UPR is upregulated in the presence of HCV E1E2 Env expression.

Knock-Down of ATF3 Expression Alleviates the Inhibitory Effects of E1E2 HCV Env on HIV-1 LTR Activity

Based on the above finding that ATF3 (a major component to the ER stress pathway) was significantly up-regulated in the presence of E1E2 we aimed to identify whether knocking-down the expression of this specific gene could modulate the E1E2 inhibitory effect observed. This is also linked with previous reports that ATF3 negatively regulates NF-κB activity (66, 67), To this end, 293T cells were transfected with three independent shRNA constructs targeting ATF3 in comparison to either a pCDNA control or ATF3 scrambled shRNA plasmid. Initially, to ensure that transfection of the shRNA constructs was not toxic to the cells, viability following transfection was measured (**Supplementary Figure 5C**). Inhibition of ATF3 production was demonstrated by Western blot analysis, which revealed reduced ATF3 expression in the presence of the shRNA constructs but not in the presence of control constructs such as scrambled shRNA and pCDNA (**Supplementary Figure 6A**).

To identify whether knocking-down ATF3 could modulate NF-κB dependent responses we transfected the above generated ATF3 knock-down cells with HIV-1 LTR-Luc (NF-κB dependent) and Tat expression plasmids and measured Luc

FIGURE 6 | Genes associated with endoplasmic reticulum stress are upregulated in the presence of E1E2. **(A)** Percentage of reads mapped to HCV genome in pCDNA (n = 4) or E1E2 (n = 6) transfected 293T cells, using Kraken2. **(B)** Volcano plot highlighting the significantly upregulated genes, based on Log2 fold change >1 or -Log10 adjusted P-value above 1.3 (P=0.05). **(C)** Ridgeplot showing top 10 biological processes that are enriched in our dataset. Differentially expressed genes are involved in misfolded protein binding and endoplasmic reticulum stress.

FIGURE 7 | Expression of NF-κB associated or HIV-1 transcription factor genes. Expression of NF-κB associated or HIV-1 transcription factor genes from normalised RNAseq libraries of 293T cells expressing E1E2 (n = 6) or pCDNA (n = 4), expressed as counts per million (CPM) **(A)** NF-κB1, **(B)** Jun, **(C)** SP1 and **(D)** RelA. Significance determined by Voom/Limma differential gene expression analysis. ns - not significant.

activity 48 h later. Pre-transfection with the three ATF3 directed shRNA plasmids provided a higher level of Luc activity than with control plasmid alone (P<0.05) (**Supplementary Figure 6B**). To assess the effect of E1E2 expression cells were similarly pre-transfected independently with the three ATF3 shRNA, or scrambled shRNA plasmids, before being transfected with E1E2, HIV-1 LTR-Luc and Tat expression plasmids and with Luc activity subsequently measured. When cells were pre-transfected with the scrambled shRNA then the typical profile of E1E2 down-modulation of LTR expression was observed (**Supplementary Figures 6C–E**, shown in red). Whereas, Knock-down of ATF3 expression was shown to negate the HCV E1E2 inhibitory effect on HIV-1 LTR activity (P<0.05) when pre-transfecting with ATF3 shRNA 1 (**Supplementary Figure 6C**, shown in green), ATF3 shRNA 2 (**Supplementary Figure 6D**, shown in green) and ATF3 shRNA 3 plasmids (**Supplementary Figure 6E**, shown in green). This result demonstrates that knocking-down ATF3 expression, one of the major components of the ER stress pathway, alleviates the inhibitory effect of E1E2 on down-modulating HIV-1 LTR activity and induced NF-κB responses. The results additionally suggest that basal expression levels of ATF3 can influence HIV-1 LTR expression activity independent of E1E2 expression.
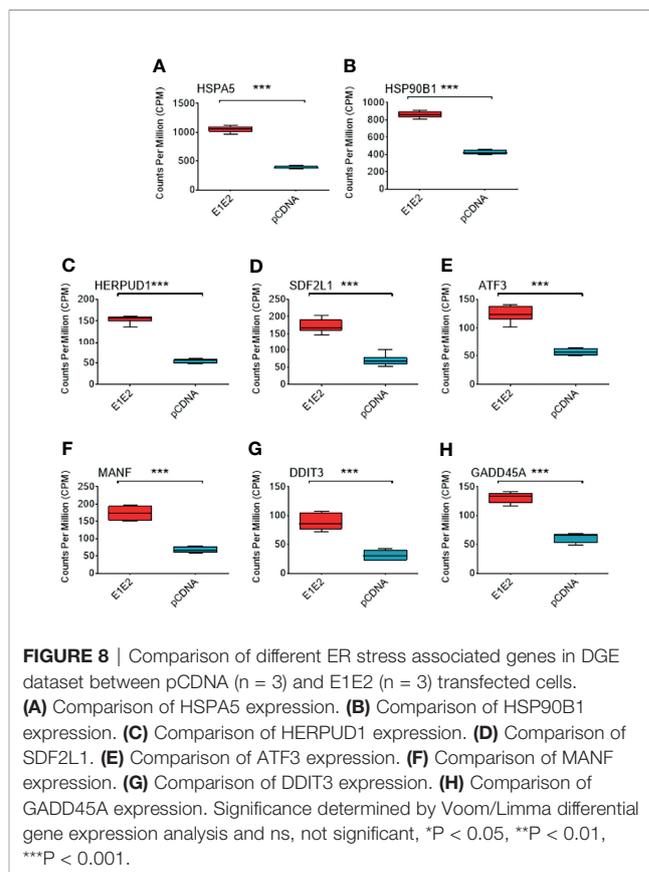
DISCUSSION

The work presented here demonstrates that the HCV E1E2 Env glycoproteins can modulate HIV-1 LTR through downregulation of NF-κB mediated immune signalling pathways. The findings presented here provides a proof-of-concept where a novel pathway exists whereby a viral Env protein (HCV) can

modulate NF-κB signalling, potentially leading to pronounced effects on an array of biological phenomena.

We have demonstrated an increased effect by sE2 alone to down-modulate HIV-1 LTR activity. Soluble E2 (sE2) has been used previously as a means to map antibody epitopes (68), CD81-related entry mechanisms (69) and DC/L-SIGN-mediated receptor binding (70). Whilst it is unclear whether sE2 is produced as a soluble glycoprotein during infection, E2 can be found in the cytoplasm of infected cells whereby it can modulate intracellular signalling pathways (expanded upon below).

The Role of E1E2 or sE2 as a Transcription Regulatory Factor

HCV E2 has previously been documented to be capable of modulating several intracellular signalling pathways, including the MAPK/ERK (71), PI3/AKT (72) and PKR/eIF2 pathways which lead to an increase in cell proliferation and survival as well as a means to enhance viral infectivity. E2 has also been shown to inhibit other signalling pathways including T-cell signalling in a cross-genotypic RNA dependant manner by reducing Lck phosphorylation (73). This in turn was shown to prevent downstream TCR signalling. Since the PKR, Lck and PI3K-AKT pathways can indirectly influence NF-κB signalling (74) this suggests a global means by which sE2 can influence cellular transcription. Similarly, here we demonstrate that sE2, either alone or as part of the E1E2 heterodimer, may also modulate the

FIGURE 8 | Comparison of different ER stress associated genes in DGE dataset between pCDNA (n = 3) and E1E2 (n = 3) transfected cells. **(A)** Comparison of HSPA5 expression. **(B)** Comparison of HSP90B1 expression. **(C)** Comparison of HERPUD1 expression. **(D)** Comparison of SDF2L1. **(E)** Comparison of ATF3 expression. **(F)** Comparison of MANF expression. **(G)** Comparison of DDIT3 expression. **(H)** Comparison of GADD45A expression. Significance determined by Voom/Limma differential gene expression analysis and ns, not significant, *P < 0.05, **P < 0.01, ***P < 0.001.

NF-κB pathway, either directly or indirectly through stimulation of inhibitory pathways.

A Potential Mechanism for HCV Derived Modulation of NF-κB Activity

Three members of the NF-κB family were detected exclusively [RelA and NF-κB2 (p100, the precursor form of p52)] or more abundantly [NF-κB1 (p105, precursor form of p50)] in the HIV-1-LTR pull-down performed in the absence of E1E2. This suggests that, although the expression (**Figure 7D** and **Supplementary Figure 2B**) of RelA is comparable in the presence or absence of E1E2, E1E2 inhibits NF-κB binding specifically to the HIV-1 LTR. Although speculative, one can hypothesize that E1E2 inhibits a RelA-targeting kinase, such as ERK, thereby modifying the DNA-binding affinity of NF-κB specifically for the kB sequence present in the LTR. Indeed, post-translation modifications of NF-κB subunits determine the sequence-specific binding of this transcription factor (75). Alternatively, the absence of HIV1-LTR-bound NF-κB might be due to the absence of the other protein partners detected in the pull-down in the absence of E1E2.

Link Between HCV and Endoplasmic Reticulum Stress

Expression of HCV proteins or replication of HCV in tissue culture models is associated with ER stress and subsequent activation of the UPR and inflammatory pathways due to the dependence on the ER for viral replication (35, 42, 76, 77). Several studies have suggested that activation of the UPR in HCV infected cells contributes to pathogenesis, including through increased liver fibrosis *via* transforming growth factor β1 (TGF-β1) induction (78) and development of insulin resistance and type 2 diabetes mellitus (79, 80). In line with these findings, we have shown that ER stress response pathways are significantly upregulated in the presence of E1E2. This supports studies which indicate E1E2 Env expression is a potent activator of ER stress (41, 42). Follow on experiments analysing more specifically the promoter regions of the ER stress dysregulated mRNA genes in the presence of E1E2 or the factors binding to these specific promoters may provide an indication as to whether altered expression of mRNA is due to E1E2 binding or the binding of other dysregulated TF induced by E1E2 expression.

The UPR is a signalling cascade that is activated when misfolded proteins accumulate in the ER and is detected by three molecular sensors: IRE1 (inositol-requiring 1α), PERK (double-stranded RNA-dependent protein kinase (PKR)-like ER kinase) and ATF6 (activating transcription factor 6) (34, 35). The activation of the UPR ultimately leads to restoration of cellular homeostasis by increasing the folding capacity of the ER and reducing protein synthesis by the upregulation of UPR effector proteins such as CHOP (DDIT3), BiP (HSPA5) and X-box binding protein 1 (XBP1) (81).

There is significant and complex interaction between the UPR and the cellular transcription machinery and evidence suggests that the UPR may cause both positive and negative regulation of NF-κB, depending on the specific conditions and the timing of the response, as reviewed (82, 83). We provide evidence that E1E2-mediated ER stress may lead to a reduction in NF-κB-dependent HIV-LTR activation, though expression of NF-κB genes were not differentially expressed in our analysis. This E1E2-associated down-modulation may therefore be *via* direct or indirect interaction with UPR effector proteins. One potential regulator is ATF3, a transcription factor that is involved in the host response to inflammation, infection and cancer (84–87). Several reports propose that ATF3 is a negative regulator of NF-κB mediated pro-inflammatory responses (88–90), including a study which showed elevated levels of immune activation through NF-κB signalling in *Drosophila melanogaster* ATF3 knockout mutants (91). A recent study indicates that ATF3 is a hub of transcriptional activity in HCV infected cells, suggesting a key role for this transcription factor in HCV infection and the response to cell stress (92). Importantly, research has shown that ATF3 directly binds the p65 NF-κB subunit, and that inhibition of ATF3 was associated with increased NF-κB activity (66). Taken together, these studies may indicate a mechanism by which HCV E1E2 activates the UPR, leading to overexpression of ATF3, a negative regulator of NF-κB. Indeed, we showed, through short hairpin RNAs targeting ATF3 transcripts, that inhibition of ATF3 expression was able to both enhance basal activation of the LTR as well as alleviate the effect of E1E2. These results suggest that E1E2 expression activates pathways that disrupt NF-κB signalling, specifically the stress response gene ATF3, and that this effect may be important in HCV mediated immune regulation. The precise mechanism *via* which the down-modulation of ATF3 leads to the down-modulation of NF-κB activity needs to be further elucidated but an association with ER stress has been demomstrated.

As the abundance of precursor proteins p100 and p105 were lower in the E1E2 containing sample, it would suggest that E1E2 modulates the production of these proteins. This may include p100 and p105 transcription/translation, or the phosphorylation process by which each protein is released from its inhibitory state. Since E2 is a documented modulator of intracellular signalling (as described above), it is proposed that E2 may be the means by which HCV modulates NF-κB signalling (as part of the E1E2 heterodimer complex) and future *in vitro* systems should clarify this.

Impact on Latency and Other Biological Systems

Modulation of NF-κB signalling also has implications with regards to HIV-1 latency. The process of maintaining HIV-1 latency can be described as a balance between enabling infected cell survival and proliferation but preventing HIV-1 gene re-expression. To this end, HIV-1 employs multiple methods by which it maintains homeostatic cell proliferation and basal levels of transcription. With regards to NF-κB involvement these include chromatin accessibility, wherein transcription factors have access to proviral DNA to facilitate binding (93). It has been postulated that the level of chromatin accessibility can determine the required level of NF-κB binding for LTR activation (94). A number of molecules with known capacities to modulate HIV-1 latency were shown to be altered in LTR pull-

downs in the absence of E1E2 expression (XCRR5 and 6) and which have been shown to enhance early expression from the HIV-1 LTR promoter (59). Pro-inflammatory cytokines (typically activated by NF-κB) also serve to replenish the HIV-1 reservoir by reactivating viral replication, however when this response is suppressed this helps maintain a homeostatic proliferation of the cellular reservoirs (95). Additionally, NF-κB (and NFAT) acts to reverse the epigenetic inhibition related to the LTR leading to proviral transcription *via* chromatin remodelling thus abolishing the histone deacetylase and methyltransferase related regulation (96). A recent study has described a higher HIV-1 proviral reservoir being identified in individuals treated for HIV-1 who were either co-infected with HCV or who resolved their HCV infection in comparison to mono-HIV-1 infected individuals (97). This could represent a mechanism whereby HCV Env expression can lead to down-modulation of HIV-1 LTR activity and induction of viral latency, not necessarily through co-infection of the same cell but *via* other mechanisms such as cellular uptake or cell fusion. There is evidence that HIV-1 can infect cells within the liver, namely primary hepatic stellate cells (HSC) where HCV replication occurs in adjacent hepatocytes. Indeed *in vitro* culture systems have indicated that liver fibrosis induction can be enhanced in HIV-1 infected individuals through complex interactions of cell-types infected with either HIV-1 or HCV (98, 99).

The potential wide-ranging modulation of various intra-cellular signalling pathways by sE2 suggests that in addition to affecting viral activity this mechanism has the potential to modulate an array of host cell phenotypes. This would undoubtedly include regulation of immune responses or cell proliferation leading to oncogenesis. NF-κB is required as part of a pro-inflammatory response and as such sustained activation of the NF-κB pathway leads to chronic inflammation and in some cases inflammation-associated cancer such as hepatocellular carcinoma (in the case of HCV-related disease) (100). Additionally, NF-κB acts to prevent apoptosis and thus prolong cell survival leading to tumour formation as well as sustaining angiogenic and metastatic factors such as vascular-endothelial growth factor and Twist1 (101). Therefore, the effect that E2 has on NF-κB or additional intracellular pathways needs to be carefully elucidated.

Overall, it is shown that HCV E2 possesses a wide-ranging capability to influence intracellular signalling events. The research presented here also demonstrates a novel consequence of HCV/HIV-1 co-infection in which E2 down-modulates LTR activity. Given that co-infection of the same cell is rare the major consequences to these findings will lie in the effect of the HCV E2 Env protein in majorly down-modulating NF-κB mediated pro-inflammatory as well as oncogenesis pathways in HCV infected individuals.

DATA AVAILABILITY STATEMENT

Data has been deposited in NCBI's Gene Expression Omnibus and accessible through GEO Series accession number GSE163239 (https://www.ncbi.nlm.nih.gov/geo/query/acc.cgi?acc= GSE163239). All reagents generated will be available from the Lead Contact with a completed Materials Transfer Agreement.

AUTHOR CONTRIBUTIONS

GP and WP designed and perceived the study. GP, WP, JM, JB, AT and PR provided scientific input and direction as well as performing data analysis. LM, JT, AF, MD, WA and AR designed and performed experiments and undertook data analysis. JM, JB and AT provided reagents. LM and WP wrote the initial manuscript. All authors contributed to the article and approved the submitted version.

FUNDING

SUPPLEMENTARY MATERIAL

The Supplementary Material for this article can be found online at: https://www.frontiersin.org/articles/10.3389/fimmu.2022.831695/full#supplementary-material

Supplementary Figure 1 | FACS analysis of **(A)** TZM-bl cells, **(B)** TZM-bl cells and isotype control, **(C)** TZM-bl-E1E2 and **(D)** TZM-bl-sE2 stably expressing cells. The primary antibody used was AP33, a mouse monoclonal and the secondary was an anti-mouse Goat PE conjugate.

Supplementary Figure 2 | E1E2 expression modulates an array of host protein transcription factors binding the HIV-1 LTR but not modulating mRNA expression Quantitative mRNA expression of transcription factors that bind the HIV-1 LTR in the presence or absence of HCV E1E2 Env expression (n = 3). **(A)** NF-κB **(B)** RelA **(C)** IF116 and **(D)** RBMX. All graphs show mean values plotted with error bars representing standard deviation.

Supplementary Figure 3 | Overview of normalisation and quality control of differential gene expression data set including pCDNA (n = 4) and E1E2 (n = 6) transfected cells. **(A)** Distribution of read lengths in mRNA libraries. **(B)** Distribution of read qualities in mRNA libraries. **(C)** Principal component analysis highlighting separation of sample groups on principle component 1. **(D)** Distribution of gene expression (Log-CPM) prior to filtering with EdgeR. **(E)** Distribution of gene expression post-filtering with EdgeR.

Supplementary Figure 4 | Gene set enrichment analysis showing the enrichment plots and corresponding heat maps of enriched gene sets that are associated with ER stress. **(A)** SRP dependent co-translational protein targeting to membrane. **(B)** PERK regulates gene expression. **(C)** Unfolded protein response (UPR). **(D)** ATF4 activates genes in response to ER stress. **(E)** IRE1ALPHA activates chaperones.

Supplementary Figure 5 | Effect of transfection and protein expression on cell viability. **(A)** Comparison of viable cell counts in cells 293T cells and 293T-E1E2 cells that were transfected with LTR sub-type plasmids and expression constructs. **(B)** Comparison of viable cell counts in cells TZM-bl cells and TZM-bl-E1E2 cells that were transfected with LTR sub-type plasmids and expression constructs. **(C)** Comparison of cell viability when cells were transfected with ATF3 knock-down constructs including scrambled shRNA and the three ATF3 shRNA plasmids. TR

represents transfection reagent, in which the transfection process was performed in the absence of plasmid DNA. **(D)** Comparison of cell viability when cells were transfected with various envelope expression plasmids. TR represents transfection reagent, in which the transfection process was performed in the absence of plasmid DNA.

Supplementary Figure 6 | Knock-down of ATF3 expression through siRNA alleviates the inhibitory effects of E1E2 HCV Env on HIV-1 LTR activity. **(A)** Western blot showing the expression level of ATF3 in 293T cells transfected with ATF3 shRNA expression plasmids, HCV E1E2 Env and scrambled siRNA pCDNA controls (top panel) and β-actin loading control (bottom panel). **(B)** Total activation of HIV-1 LTR in 293T cells when cells were prior transfected with ATF3 shRNA expression plasmids (green bars) or pCDNA (grey bar) and scrambled shRNA (blue bar) controls (n = 3). Cells were initially transfected with siRNAs or pCDNA expression plasmid and 48h later were transfected with 50 ng LTR-Luc and 5 ng HIV-1 Tat plasmids and with Luc activity measured 48 h later from cell lysate. Letter codes used for transfection are as follows: L: LTR-luc, T: Tat, E: E1E2, P: pCDNA, A: ATF3 shRNA, S: scrambled shRNA. **(C–E)** demonstrate Luc activity from 293T cell lysates when cells were prior co-transfected with ATF3 shRNA expression plasmid and 48h later with E1E2 HCV Env, LTR-Luc and HIV-1 Tat plasmids and Luc activity measured 48h subsequently (green bars) (n = 3). Cells non-transfected with siRNA prior to E1E2 Env, LTR-Luc and HIV-1 Tat plasmid transfection were used as a positive control for monitoring the effects of E1E2 expression (red bars) and cells transfected with control LTR-Luc and HIV-1 Tat to determine basal Luc expression (grey bars). The inhibitory effects of E1E2 HCV Env on HIV-1 LTR activity is alleviated in the presence of **(C)** ATF3 shRNA 1, **(D)** ATF3 shRNA 2 and **(E)** ATF3 shRNA 3 when compared with controls. The same letter codes described above for panel B were also used for panels **(C–E)**. For all graphs, mean is plotted and error bars represent standard deviation. Kruskal-Wallis and Dunn's test were used to determine statistical significance. * P<0.05.

Supplementary Table 1 | Identification of the proteins captured by the HIV-1-LTR in the presence or absence of E1E2. Nuclear extracts proteins from TZM-bl cells transiently transfected with E1E2 plasmid ("E1E2") or with pCDNA plasmid ("control") were pulled-down with a HIV-1-LTR DNA fragment and identified by mass spectrometry. A quantitative analysis was performed to compare the normalized spectral count in E1E2 and control conditions, with a T-test comparison. The proteins are sorted by significance (p-value < 0.05). The normalized spectral count is indicated for each biological independent triplicate, as well as the merge value. Of note, technical contaminants like serum albumin, keratins, and biotin-binding proteins such as pyruvate carboxylase, methyl-crotonyl CoA carboxylase, propionyl CoA carboxylase and acetyl CoA carboxylase were removed from the protein lists.

Supplementary Table 2 | Most significantly enriched pathways from Broad Institute's GSEA software. NES represents normalised enrichment score. FDR represents false discovery rate.

REFERENCES

1. WHO. *Hepatitis C* (2021). Available at: https://www.who.int/news-room/fact-sheets/detail/hepatitis-c (Accessed January 16, 2022).

2. Yamane D, McGivern DR, Masaki T, Lemon SM. Liver Injury and Disease Pathogenesis in Chronic Hepatitis C. In: *Curr Top Microbiol Immunol*. Springer (2013) 369:263–88. doi: 10.1007/978-3-642-27340-7_11

3. Millman AJ, Nelson NP, Vellozzi C. Hepatitis C: Review of the Epidemiology, Clinical Care, and Continued Challenges in the Direct Acting Antiviral Era. *Curr Epidemiol Rep* (2017) 4:174–85. doi: 10.1007/s40471-017-0108-x

4. Allison RD, Conry-Cantilena C, Koziol D, Schechterly C, Ness P, Gibble J, et al. A 25-Year Study of the Clinical and Histologic Outcomes of Hepatitis C Virus Infection and its Modes of Transmission in a Cohort of Initially Asymptomatic Blood Donors. *J Infect Dis* (2012) 206:654–61. doi: 10.1093/infdis/jis410

5. Ivanov AV, Bartosch B, Smirnova OA, Isaguliants MG, Kochetkov SN. HCV and Oxidative Stress in the Liver. *Viruses* (2013) 5:439–69. doi: 10.3390/v5020439

6. Zaltron S, Spinetti A, Biasi L, Baiguera C, Castelli F. Chronic HCV Infection: Epidemiological and Clinical Relevance. *BMC Infect Dis* (2012) 12 Suppl 2: S2–2. doi: 10.1186/1471-2334-12-S2-S2

7. Thomson EC, Fleming VM, Main J, Klenerman P, Weber J, Eliahoo J, et al. Predicting Spontaneous Clearance of Acute Hepatitis C Virus in a Large Cohort of HIV-1-Infected Men. *Gut* (2011) 60:837–45. doi: 10.1136/gut.2010.217166

8. Santantonio T, Wiegand J, Gerlach JT. Acute Hepatitis C: Current Status and Remaining Challenges. *J Hepatol* (2008) 49:625–33. doi: 10.1016/j.jhep.2008.07.005

9. Micallef JM, Kaldor JM, Dore GJ. Spontaneous Viral Clearance Following Acute Hepatitis C Infection: A Systematic Review of Longitudinal Studies. *J Viral Hepat* (2006) 13:34–41. doi: 10.1111/j.1365-2893.2005.00651.x

10. Farci P, Shimoda A, Coiana A, Diaz G, Peddis G, Melpolder JC, et al. The Outcome of Acute Hepatitis C Predicted by the Evolution of the Viral Quasispecies. *Sci (80-)* (2000) 288:339 LP – 344. doi: 10.1126/science.288.5464.339

11. Thomas DL, Astemborski J, Rai RM, Anania FA, Schaeffer M, Galai N, et al. The Natural History of Hepatitis C Virus InfectionHost, Viral, and Environmental Factors. *JAMA* (2000) 284:450–6. doi: 10.1001/jama.284.4.450

12. Villano SA, Vlahov D, Nelson KE, Cohn S, Thomas DL. Persistence of Viremia and the Importance of Long-Term Follow-Up After Acute Hepatitis C Infection. *Hepatology* (1999) 29:908–14. doi: 10.1002/hep.510290311

13. Grebely J, Raffa JD, Lai C, Krajden M, Conway B, Tyndall MW. Factors Associated With Spontaneous Clearance of Hepatitis C Virus Among Illicit Drug Users. *Can J Gastroenterol* (2007) 21:447–51. doi: 10.1155/2007/796325

14. Operskalski EA, Mack WJ, Strickler HD, French AL, Augenbraun M, Tien PC, et al. Factors Associated With Hepatitis C Viremia in a Large Cohort of HIV-Infected and-Uninfected Women. *J Clin Virol* (2008) 41:255–63. doi: 10.1016/j.jcv.2007.08.021

15. Strasfeld L, Lo Y, Netski D, Thomas DL, Klein RS. The Association of Hepatitis C Prevalence, Activity, and Genotype With HIV Infection in a Cohort of New York City Drug Users. *J Acquir Immune Defic Syndr* (2003) 33:356–64. doi: 10.1097/00126334-200307010-00010

16. Shores NJ, Maida I, Soriano V, Núñez M. Sexual Transmission is Associated With Spontaneous HCV Clearance in HIV-Infected Patients. *J Hepatol* (2008) 49:323–8. doi: 10.1016/j.jhep.2008.04.010

17. Coppola N, Marrone A, Pisaturo M, Starace M, Signoriello G, Gentile I, et al. Role of Interleukin 28-B in the Spontaneous and Treatment-Related Clearance of HCV Infection in Patients With Chronic HBV/HCV Dual Infection. *Eur J Clin Microbiol Infect Dis* (2014) 33:559–67. doi: 10.1007/S10096-013-1985-7

18. Grebely J, Page K, Sacks-Davis R, van der Loeff MS, Rice TM, Bruneau J, et al. The Effects of Female Sex, Viral Genotype, and IL28B Genotype on Spontaneous Clearance of Acute Hepatitis C Virus Infection. *Hepatology* (2014) 59:109–20. doi: 10.1002/hep.26639

19. Grebely J, Petoumenos K, Hellard M, Matthews GV, Suppiah V, Applegate T, et al. Potential Role for Interleukin-28B Genotype in Treatment Decision-Making in Recent Hepatitis C Virus Infection. *Hepatology* (2010) 52:1216–24. doi: 10.1002/hep.23850

20. Rauch A, Gaudieri S, Thio C, Bochud P-Y. Host Genetic Determinants of Spontaneous Hepatitis C Clearance. *Pharmacogenomics* (2009) 10:1819–37. doi: 10.2217/pgs.09.121

21. Post J, Ratnarajah S, Lloyd AR. Immunological Determinants of the Outcomes From Primary Hepatitis C Infection. *Cell Mol Life Sci* (2009) 66:733–56. doi: 10.1007/s00018-008-8270-4

22. Ferreira AR, Ramos B, Nunes A, Ribeiro D. Hepatitis C Virus: Evading the Intracellular Innate Immunity. *J Clin Med* (2020) 9:790. doi: 10.3390/jcm9030790

23. Shrivastava A, Manna SK, Ray R, Aggarwal BB. Ectopic Expression of Hepatitis C Virus Core Protein Differentially Regulates Nuclear Transcription Factors. *J Virol* (1998) 72:9722–8. doi: 10.1128/JVI.72.12.9722-9728.1998

24. Nguyen H, Sankaran S, Dandekar S. Hepatitis C Virus Core Protein Induces Expression of Genes Regulating Immune Evasion and Anti-Apoptosis in Hepatocytes. *Virology* (2006) 354:58–68. doi: 10.1016/j.virol.2006.04.028

25. Joo M, Hahn YS, Kwon M, Sadikot RT, Blackwell TS, Christman JW. Hepatitis C Virus Core Protein Suppresses NF-kappaB Activation and Cyclooxygenase-2 Expression by Direct Interaction With IkappaB Kinase Beta. J Virol (2005) 79:7648–57. doi: 10.1128/JVI.79.12.7648-7657.2005

26. Sundström S, Ota S, Dimberg LY, Masucci MG, Bergqvist A. Hepatitis C Virus Core Protein Induces an Anergic State Characterized by Decreased Interleukin-2 Production and Perturbation of Mitogen-Activated Protein Kinase Responses. J Virol (2005) 79:2230 LP – 2239. doi: 10.1128/JVI.79.4.2230-2239.2005

27. Dominguez-Villar M, Fernandez-Ponce C, Munoz-Suano A, Gomez E, Rodríguez-Iglesias M, Garcia-Cozar F. Up-Regulation of FOXP3 and Induction of Suppressive Function in CD4+ Jurkat T-Cells Expressing Hepatitis C Virus Core Protein. Clin Sci (2012) 123:15–27. doi: 10.1042/CS20110631

28. Domínguez-Villar M, Muñoz-Suano A, Anaya-Baz B, Aguilar S, Novalbos JP, Giron JA, et al. Hepatitis C Virus Core Protein Up-Regulates Anergy-Related Genes and a New Set of Genes, Which Affects T Cell Homeostasis. J Leukoc Biol (2007) 82:1301–10. doi: 10.1189/jlb.0507335

29. Kaukinen P, Sillanpää M, Kotenko S, Lin R, Hiscott J, Melén K, et al. Hepatitis C Virus NS2 and NS3/4A Proteins are Potent Inhibitors of Host Cell Cytokine/Chemokine Gene Expression. Virol J (2006) 3:66. doi: 10.1186/1743-422X-3-66

30. Li K, Foy E, Ferreon JC, Nakamura M, Ferreon ACM, Ikeda M, et al. Immune Evasion by Hepatitis C Virus NS3/4A Protease-Mediated Cleavage of the Toll-Like Receptor 3 Adaptor Protein TRIF. Proc Natl Acad Sci (2005) 102:2992–7. doi: 10.1073/pnas.0408824102

31. Foy E, Li K, Wang C, Sumpter R, Ikeda M, Lemon SM, et al. Regulation of Interferon Regulatory Factor-3 by the Hepatitis C Virus Serine Protease. Sci (80-) (2003) 300:1145–8. doi: 10.1126/science.1082604

32. Gagné B, Tremblay N, Park AY, Baril M, Lamarre D. Importin β1 Targeting by Hepatitis C Virus NS3/4A Protein Restricts IRF3 and NF-κb Signaling of IFNB1 Antiviral Response. Traffic (2017) 18:362–77. doi: 10.1111/tra.12480

33. Bellecave P, Sarasin-Filipowicz M, Donzé O, Kennel A, Gouttenoire J, Meylan E, et al. Cleavage of Mitochondrial Antiviral Signaling Protein in the Liver of Patients With Chronic Hepatitis C Correlates With a Reduced Activation of the Endogenous Interferon System. Hepatology (2010) 51:1127–36. doi: 10.1002/hep.23426

34. Chan S-W. Unfolded Protein Response in Hepatitis C Virus Infection. Front Microbiol (2014) 5:233:233. doi: 10.3389/fmicb.2014.00233

35. Ríos-Ocampo WA, Navas M-C, Faber KN, Daemen T, Moshage H. The Cellular Stress Response in Hepatitis C Virus Infection: A Balancing Act to Promote Viral Persistence and Host Cell Survival. Virus Res (2019) 263:1–8. doi: 10.1016/j.virusres.2018.12.013

36. Ke P-Y, Chen SS-L. Activation of the Unfolded Protein Response and Autophagy After Hepatitis C Virus Infection Suppresses Innate Antiviral Immunity In Vitro. J Clin Invest (2011) 121:37–56. doi: 10.1172/JCI41474

37. Tanida I, Fukasawa M, Ueno T, Kominami E, Wakita T, Hanada K. Knockdown of Autophagy-Related Gene Decreases the Production of Infectious Hepatitis C Virus Particles. Autophagy (2009) 5:937–45. doi: 10.4161/auto.5.7.9243

38. Sir D, Chen W-L, Choi J, Wakita T, Yen TSB, Ou J-HJ. Induction of Incomplete Autophagic Response by Hepatitis C Virus via the Unfolded Protein Response. Hepatology (2008) 48:1054–61. doi: 10.1002/hep.22464

39. Dreux M, Gastaminza P, Wieland SF, Chisari FV. The Autophagy Machinery is Required to Initiate Hepatitis C Virus Replication. Proc Natl Acad Sci USA (2009) 106:14046–51. doi: 10.1073/pnas.0907344106

40. Chan S-W, Egan PA. Hepatitis C Virus Envelope Proteins Regulate CHOP via Induction of the Unfolded Protein Response. FASEB J (2005) 19:1510–2. doi: 10.1096/fj.04-3455fje

41. Pavio N, Romano PR, Graczyk TM, Feinstone SM, Taylor DR. Protein Synthesis and Endoplasmic Reticulum Stress Can Be Modulated by the Hepatitis C Virus Envelope Protein E2 Through the Eukaryotic Initiation Factor 2α Kinase PERK. J Virol (2003) 77:3578 LP – 3585. doi: 10.1128/JVI.77.6.3578-3585.2003

42. Chan S-W, Egan PA. Effects of Hepatitis C Virus Envelope Glycoprotein Unfolded Protein Response Activation on Translation and Transcription. Arch Virol (2009) 154:1631. doi: 10.1007/s00705-009-0495-5

43. Lavie M, Goffard A, Dubuisson J. HCV Glycoproteins: Assembly of a Functional E1–E2 Heterodimer. Hepat C Viruses Genomes Mol Biol (2006). doi: 10.1007/S00705-009-0495-5

44. Tarr AW, Urbanowicz RA, Hamed MR, Albecka A, McClure CP, Brown RJP, et al. Hepatitis C Patient-Derived Glycoproteins Exhibit Marked Differences in Susceptibility to Serum Neutralizing Antibodies: Genetic Subtype Defines Antigenic But Not Neutralization Serotype. J Virol (2011) 85:4246–57. doi: 10.1128/JVI.01332-10

45. Lavillette D, Tarr AW, Voisset C, Donot P, Bartosch B, Bain C, et al. Characterization of Host-Range and Cell Entry Properties of the Major Genotypes and Subtypes of Hepatitis C Virus. Hepatology (2005) 41:265–74. doi: 10.1002/hep.20542

46. Tacheny A, Michel S, Dieu M, Payen L, Arnould T, Renard P. Unbiased Proteomic Analysis of Proteins Interacting With the HIV-1 5'LTR Sequence: Role of the Transcription Factor Meis. Nucleic Acids Res (2012) 40:e168–8. doi: 10.1093/nar/gks733

47. Wood DE, Lu J, Langmead B. Improved Metagenomic Analysis With Kraken 2. Genome Biol (2019) 20:257. doi: 10.1186/s13059-019-1891-0

48. Li H. Minimap2: Pairwise Alignment for Nucleotide Sequences. Bioinformatics (2018) 34:3094–100. doi: 10.1093/bioinformatics/bty191

49. Liao Y, Smyth GK, Shi W. Featurecounts: An Efficient General Purpose Program for Assigning Sequence Reads to Genomic Features. Bioinformatics (2013) 30:923–30. doi: 10.1093/bioinformatics/btt656

50. Robinson MD, McCarthy DJ, Smyth GK. Edger: A Bioconductor Package for Differential Expression Analysis of Digital Gene Expression Data. Bioinformatics (2009) 26:139–40. doi: 10.1093/bioinformatics/btp616

51. Law CW, Chen Y, Shi W, Smyth GK. Voom: Precision Weights Unlock Linear Model Analysis Tools for RNA-Seq Read Counts. Genome Biol (2014) 15:R29. doi: 10.1186/gb-2014-15-2-r29

52. Ritchie ME, Phipson B, Wu D, Hu Y, Law CW, Shi W, et al. Limma Powers Differential Expression Analyses for RNA-Sequencing and Microarray Studies. Nucleic Acids Res (2015) 43:e47–7. doi: 10.1093/nar/gkv007

53. Yu G, Wang L-G, Han Y, He Q-Y. Clusterprofiler: An R Package for Comparing Biological Themes Among Gene Clusters. Omi A J Integr Biol (2012) 16:284–7. doi: 10.1089/omi.2011.0118

54. Subramanian A, Tamayo P, Mootha VK, Mukherjee S, Ebert BL, Gillette MA, et al. Gene Set Enrichment Analysis: A Knowledge-Based Approach for Interpreting Genome-Wide Expression Profiles. Proc Natl Acad Sci (2005) 102:15545 LP – 15550. doi: 10.1073/pnas.0506580102

55. Janz M, Hummel M, Truss M, Wollert-Wulf B, Mathas S, Jöhrens K, et al. Classical Hodgkin Lymphoma is Characterized by High Constitutive Expression of Activating Transcription Factor 3 (ATF3), Which Promotes Viability of Hodgkin/Reed-Sternberg Cells. Blood (2006) 107:2536–9. doi: 10.1182/blood-2005-07-2694

56. Harrich D, Garcia J, Wu F, Mitsuyasu R, Gonazalez J, Gaynor R. Role of SP1-Binding Domains in In Vivo Transcriptional Regulation of the Human Immunodeficiency Virus Type 1 Long Terminal Repeat. J Virol (1989) 63:2585–91. doi: 10.1128/jvi.63.6.2585-2591.1989

57. Rohr O, Schwartz C, Hery C, Aunis D, Tardieu M, Schaeffer E. The Nuclear Receptor Chicken Ovalbumin Upstream Promoter Transcription Factor Interacts With HIV-1 Tat and Stimulates Viral Replication in Human Microglial Cells. J Biol Chem (2000) 275:2654–60. doi: 10.1074/jbc.275.4.2654

58. Hwang S-B, Burbach JPH, Chang C. TR4 Orphan Receptor Crosstalks to Chicken Ovalbumin Upstream Protein-Transcription Factor and Thyroid Hormone Receptor to Induce the Transcriptional Activity of the Human Immunodeficiency Virus Type 1 Long-Terminal Repeat. Endocrine (1998) 8:169–75. doi: 10.1385/ENDO:8:2:169

59. Manic G, Maurin-Marlin A, Laurent F, Vitale I, Thierry S, Delelis O, et al. Impact of the Ku Complex on HIV-1 Expression and Latency. PloS One (2013) 8:e69691. doi: 10.1371/journal.pone.0069691

60. Hotter D, Bosso M, Jønsson KL, Krapp C, Stürzel CM, Das A, et al. IFI16 Targets the Transcription Factor Sp1 to Suppress HIV-1 Transcription and Latency Reactivation. Cell Host Microbe (2019) 25:858–72. doi: 10.1016/j.chom.2019.05.002

61. St. Gelais C, Roger J, Wu L. Non-POU Domain-Containing Octamer-Binding Protein Negatively Regulates HIV-1 Infection in CD4+ T Cells. AIDS Res Hum Retroviruses (2015) 31:806–16. doi: 10.1089/aid.2014.0313

62. Yan J, Shun M-C, Zhang Y, Hao C, Skowronski J. HIV-1 Vpr Counteracts HLTF-Mediated Restriction of HIV-1 Infection in T Cells. *Proc Natl Acad Sci* (2019) 116:9568–77. doi: 10.1073/pnas.1818401116

63. Parent M, Yung TMC, Rancourt A, Ho ELY, Vispé S, Suzuki-Matsuda F, et al. Poly (ADP-Ribose) Polymerase-1 is a Negative Regulator of HIV-1 Transcription Through Competitive Binding to TAR RNA With Tat-Positive Transcription Elongation Factor B (P-TEFb) Complex. *J Biol Chem* (2005) 280:448–57. doi: 10.1074/jbc.M408435200

64. Kameoka M, Nukuzuma S, Itaya A, Tanaka Y, Ota K, Ikuta K, et al. RNA Interference Directed Against Poly (ADP-Ribose) Polymerase 1 Efficiently Suppresses Human Immunodeficiency Virus Type 1 Replication in Human Cells. *J Virol* (2004) 78:8931–4. doi: 10.1128/JVI.78.16.8931-8934.2004

65. Ma L, Jiang Q-A, Sun L, Yang X, Huang H, Jin X, et al. X-Linked RNA-Binding Motif Protein Modulates HIV-1 Infection of CD4+ T Cells by Maintaining the Trimethylation of Histone H3 Lysine 9 at the Downstream Region of the 5′ Long Terminal Repeat of HIV Proviral DNA. *MBio* (2020) 11(2):e03424–19. doi: 10.1128/mBio.03424-19

66. Kwon J-W, Kwon H-K, Shin H-J, Choi Y-M, Anwar MA, Choi S. Activating Transcription Factor 3 Represses Inflammatory Responses by Binding to the P65 Subunit of NF-κb. *Sci Rep* (2015) 5:14470. doi: 10.1038/srep14470

67. Jung DH, Kim K-H, Byeon HE, Park HJ, Park B, Rhee D-K, et al. Involvement of ATF3 in the Negative Regulation of iNOS Expression and NO Production in Activated Macrophages. *Immunol Res* (2015) 62:35–45. doi: 10.1007/s12026-015-8633-5

68. Owsianka A, Tarr AW, Juttla VS, Lavillette D, Bartosch B, Cosset F-L, et al. Monoclonal Antibody AP33 Defines a Broadly Neutralizing Epitope on the Hepatitis C Virus E2 Envelope Glycoprotein. *J Virol* (2005) 79:11095–104. doi: 10.1128/JVI.79.17.11095-11104.2005

69. Heo T-H, Lee S-M, Bartosch B, Cosset F-L, Kang C-Y. Hepatitis C Virus E2 Links Soluble Human CD81 and SR-B1 Protein. *Virus Res* (2006) 121:58–64. doi: 10.1016/j.virusres.2006.04.002

70. Lozach P-Y, Lortat-Jacob H, De Lavalette ADL, Staropoli I, Foung S, Amara A, et al. DC-SIGN and L-SIGN are High Affinity Binding Receptors for Hepatitis C Virus Glycoprotein E2. *J Biol Chem* (2003) 278:20358–66. doi: 10.1074/jbc.M301284200

71. Zhao L, Zhao P, Chen Q, Ren H, Pan W, Qi Z. Mitogen-Activated Protein Kinase Signalling Pathways Triggered by the Hepatitis C Virus Envelope Protein E2: Implications for the Prevention of Infection. *Cell Prolif* (2007) 40:508–21. doi: 10.1111/j.1365-2184.2007.00453.x

72. Liu Z, Tian Y, Machida K, Lai MMC, Luo G, Foung SKH, et al. Transient Activation of the PI3K-AKT Pathway by Hepatitis C Virus to Enhance Viral Entry. *J Biol Chem* (2012) 287:41922–30. doi: 10.1074/jbc.M112.414789

73. Bhattarai N, McLinden JH, Xiang J, Kaufman TM, Stapleton JT. Conserved Motifs Within Hepatitis C Virus Envelope (E2) RNA and Protein Independently Inhibit T Cell Activation. *PloS Pathog* (2015) 11:e1005183. doi: 10.1371/journal.ppat.1005183

74. Deb A, Haque SJ, Mogensen T, Silverman RH, Williams BRG. RNA-Dependent Protein Kinase PKR is Required for Activation of NF-κb by IFN-γ in a STAT1-Independent Pathway. *J Immunol* (2001) 166:6170–80. doi: 10.4049/jimmunol.166.10.6170

75. Christian F, Smith EL, Carmody RJ. The Regulation of NF-κb Subunits by Phosphorylation. *Cells* (2016) 5:12. doi: 10.3390/cells5010012

76. Joyce MA, Walters K-A, Lamb S-E, Yeh MM, Zhu C, Kneteman N, et al. HCV Induces Oxidative and ER Stress, and Sensitizes Infected Cells to Apoptosis in SCID/Alb-uPA Mice. *PloS Pathog* (2009) 5:e1000291–e1000291. doi: 10.1371/journal.ppat.1000291

77. Merquiol E, Uzi D, Mueller T, Goldenberg D, Nahmias Y, Xavier RJ, et al. HCV Causes Chronic Endoplasmic Reticulum Stress Leading to Adaptation and Interference With the Unfolded Protein Response. *PloS One* (2011) 6:e24660. doi: 10.1371/journal.pone.0024660

78. Chusri P, Kumthip K, Hong J, Zhu C, Duan X, Jilg N, et al. HCV Induces Transforming Growth Factor β1 Through Activation of Endoplasmic Reticulum Stress and the Unfolded Protein Response. *Sci Rep* (2016) 6:22487. doi: 10.1038/srep22487

79. Bernsmeier C, Duong FHT, Christen V, Pugnale P, Negro F, Terracciano L, et al. Virus-Induced Over-Expression of Protein Phosphatase 2A Inhibits Insulin Signalling in Chronic Hepatitis C. *J Hepatol* (2008) 49:429–40. doi: 10.1016/j.jhep.2008.04.007

80. Yao W, Cai H, Li X, Li T, Hu L, Peng T. Endoplasmic Reticulum Stress Links Hepatitis C Virus RNA Replication to Wild-Type PGC-1α/Liver-Specific PGC-1α Upregulation. *J Virol* (2014) 88:8361 LP – 8374. doi: 10.1128/JVI.01202-14

81. Hetz C. The Unfolded Protein Response: Controlling Cell Fate Decisions Under ER Stress and Beyond. *Nat Rev Mol Cell Biol* (2012) 13:89–102. doi: 10.1038/nrm3270

82. Schmitz ML, Shaban MS, Albert BV, Gökçen A, Kracht M. The Crosstalk of Endoplasmic Reticulum (ER) Stress Pathways With NF-κb: Complex Mechanisms Relevant for Cancer, Inflammation and Infection. *Biomedicines* (2018) 6:58. doi: 10.3390/biomedicines6020058

83. Tam AB, Mercado EL, Hoffmann A, Niwa M. ER Stress Activates NF-κb by Integrating Functions of Basal IKK Activity, IRE1 and PERK. *PloS One* (2012) 7:e45078. doi: 10.1371/journal.pone.0045078

84. Mayer SI, Dexheimer V, Nishida E, Kitajima S, Thiel G. Expression of the Transcriptional Repressor ATF3 in Gonadotrophs Is Regulated by Egr-1, CREB, and ATF2 After Gonadotropin-Releasing Hormone Receptor Stimulation. *Endocrinology* (2008) 149:6311–25. doi: 10.1210/en.2008-0251

85. Gilchrist M, Henderson WRJr., Clark AE, Simmons RM, Ye X, Smith KD, et al. Activating Transcription Factor 3 Is a Negative Regulator of Allergic Pulmonary Inflammation. *J Exp Med* (2008) 205:2349–57. doi: 10.1084/jem.20072254

86. Wu X, Nguyen B-C, Dziunycz P, Chang S, Brooks Y, Lefort K, et al. Opposing Roles for Calcineurin and ATF3 in Squamous Skin Cancer. *Nature* (2010) 465:368–72. doi: 10.1038/nature08996

87. Pelzer AE, Bektic J, Haag P, Berger AP, Pycha A, Schäfer G, et al. The Expression of Transcription Factor Activating Transcription Factor 3 in the Human Prostate and its Regulation by Androgen in Prostate Cancer. *J Urol* (2006) 175:1517–22. doi: 10.1016/S0022-5347(05)00651-8

88. Labzin LI, Schmidt SV, Masters SL, Beyer M, Krebs W, Klee K, et al. ATF3 Is a Key Regulator of Macrophage IFN Responses. *J Immunol* (2015) 195:4446 LP – 4455. doi: 10.4049/jimmunol.1500204

89. Hua B, Tamamori-Adachi M, Luo Y, Tamura K, Morioka M, Fukuda M, et al. Kitajima S. A Splice Variant of Stress Response Gene ATF3 Counteracts NF-κb-Dependent Anti-Apoptosis Through Inhibiting Recruitment of CREB-Binding Protein/p300 Coactivator. *J Biol Chem* (2006) 281:1620–9. doi: 10.1074/jbc.M508471200

90. Park S-H, Do KH, Choi HJ, Kim J, Kim K-H, Park J, et al. Novel Regulatory Action of Ribosomal Inactivation on Epithelial Nod2-Linked Proinflammatory Signals in Two Convergent ATF3-Associated Pathways. *J Immunol* (2013) 191:5170–81. doi: 10.4049/jimmunol.1301145

91. Rynes J, Donohoe CD, Frommolt P, Brodesser S, Jindra M, Uhlirova M. Activating Transcription Factor 3 Regulates Immune and Metabolic Homeostasis. *Mol Cell Biol* (2012) 32:3949 LP – 3962. doi: 10.1128/MCB.00429-12

92. Liu J, Wang B, Wang W, Sun M, Li Y, Jia X, et al. Computational Networks of Activating Transcription Factor 3 Gene in Huh7 Cell Lines and Hepatitis C Virus-Infected Huh7 Cell Lines. *Mol Med Rep* (2015) 12:1239–46. doi: 10.3892/mmr.2015.3548

93. Tsompana M, Buck MJ. Chromatin Accessibility: A Window Into the Genome. *Epigenet Chromatin* (2014) 7:1–16. doi: 10.1186/1756-8935-7-33

94. Miller-Jensen K, Dey SS, Pham N, Foley JE, Arkin AP, Schaffer DV. Chromatin Accessibility at the HIV LTR Promoter Sets a Threshold for NF-κb Mediated Viral Gene Expression. *Integr Biol* (2012) 4:661–71. doi: 10.1039/c2ib20009k

95. Dahabieh MS, Battivelli E, Verdin E. Understanding HIV Latency: The Road to an HIV Cure. *Annu Rev Med* (2015) 66:407–21. doi: 10.1146/annurev-med-092112-152941

96. Mbonye U, Karn J. Transcriptional Control of HIV Latency: Cellular Signaling Pathways, Epigenetics, Happenstance and the Hope for a Cure. *Virology* (2014) 454:328–39. doi: 10.1016/j.virol.2014.02.008

97. López-Huertas MR, Palladino C, Garrido-Arquero M, Esteban-Cartelle B, Sánchez-Carrillo M, Martínez-Román P, et al. HCV-Coinfection is Related to an Increased HIV-1 Reservoir Size in cART-Treated HIV Patients: A Cross-Sectional Study. *Sci Rep* (2019) 9:5606. doi: 10.1038/s41598-019-41788-9

98. Tuyama AC, Hong F, Saiman Y, Wang C, Ozkok D, Mosoian A, et al. Human Immunodeficiency Virus (HIV)-1 Infects Human Hepatic Stellate Cells and Promotes Collagen I and Monocyte Chemoattractant Protein-1 Expression: Implications for the Pathogenesis of HIV/hepatitis C Virus-Induced Liver Fibrosis. *Hepatology* (2010) 52:612–22. doi: 10.1002/hep.23679

99. Akil A, Endsley M, Shanmugam S, Saldarriaga O, Somasunderam A, Spratt H, et al. Fibrogenic Gene Expression in Hepatic Stellate Cells Induced by HCV and HIV Replication in a Three Cell Co-Culture Model System. *Sci Rep* (2019) 9:568. doi: 10.1038/s41598-018-37071-y

100. Pikarsky E, Porat RM, Stein I, Abramovitch R, Amit S, Kasem S, et al. NF-κb Functions as a Tumour Promoter in Inflammation-Associated Cancer. *Nature* (2004) 431:461–6. doi: 10.1038/nature02924

101. Xia Y, Shen S, Verma IM. NF-κb, an Active Player in Human Cancers. *Cancer Immunol Res* (2014) 2:823–30. doi: 10.1158/2326-6066.CIR-14-0112

Conflict of Interest: The authors declare that the research was conducted in the absence of any commercial or financial relationships that could be construed as a potential conflict of interest.